Redox Biology 61 (2023) 102634

Contents lists available at ScienceDirect

Redox Biology

journal homepage: www.elsevier.com/locate/redox

DNA repair byproduct 8-oxoguanine base promotes myoblast differentiation

Xu Zheng [a,b], Wenhe Zhang [d], Yinchao Hu [a,b], Zhexuan Zhao [a,b], Jiaxin Wu [a,b], Xiaoqing Zhang [a,b], Fengqi Hao [a,c], Jinling Han [a,b], Jing Xu [a,b], Wenjing Hao [e], Ruoxi Wang [f], Meihong Tian [c], Zsolt Radak [g], Yusaku Nakabeppu [h], Istvan Boldogh [i], Xueqing Ba [a,b,*]

[a] The Key Laboratory of Molecular Epigenetics of Ministry of Education, Northeast Normal University, Changchun, Jilin, 130024, China
[b] School of Life Sciences, Northeast Normal University, Changchun, Jilin, 130024, China
[c] School of Physical Education, Northeast Normal University, Changchun, Jilin, 130024, China
[d] Changchun Institute of Applied Chemistry, Chinese Academy of Sciences, Changchun, Jilin 130022, China
[e] Institute of Genetics and Developmental Biology, Chinese Academy of Sciences, Beijing, 100101, China
[f] Institute of Biomedical Sciences, College of Life Sciences, Key Laboratory of Animal Resistance Biology of Shandong Province, Shandong Normal University, Jinan, Shandong, 250014, China
[g] Research Institute of Sport Science, University of Physical Education, H-1123, Budapest, Hungary
[h] Division of Neurofunctional Genomics, Department of Immunobiology and Neuroscience, Medical Institute of Bioregulation, Kyushu University, Fukuoka, 812-8582, Japan
[i] Department of Microbiology and Immunology, University of Texas Medical Branch at Galveston, Galveston, TX77555, USA

ARTICLE INFO

Keywords:
8-Oxo-7
8-Dihydroguanine (8-oxoG)
8-oxoG glycosylase 1 (OGG1)
Guanine nucleotide exchange factor (GEF)
Myoblast
Myogenic differentiation

ABSTRACT

Muscle contraction increases the level of reactive oxygen species (ROS), which has been acknowledged as key signaling entities in muscle remodeling and to underlie the healthy adaptation of skeletal muscle. ROS inevitably endows damage to various cellular molecules including DNA. DNA damage ought to be repaired to ensure genome integrity; yet, how DNA repair byproducts affect muscle adaptation remains elusive. Here, we showed that exercise elicited the generation of 8-oxo-7,8-dihydroguanine (8-oxoG), that was primarily found in mitochondrial genome of myofibers. Upon exercise, TA muscle's 8-oxoG excision capacity markedly enhanced, and in the interstitial fluid of TA muscle from the post-exercise mice, the level of free 8-oxoG base was significantly increased. Addition of 8-oxoG to myoblasts triggered myogenic differentiation via activating Ras-MEK-MyoD signal axis. 8-Oxoguanine DNA glycosylase1 (OGG1) silencing from cells or *Ogg1* KO from mice decreased Ras activation, ERK phosphorylation, MyoD transcriptional activation, myogenic regulatory factors gene (MRFs) expression. In reconstruction experiments, exogenously added 8-oxoG base enhanced the expression of MRFs and accelerated the recovery of the injured skeletal muscle. Collectively, these data not only suggest that DNA repair metabolite 8-oxoG function as a signal entity for muscle remodeling and contribute to exercise-induced adaptation of skeletal muscle, but also raised the potential for utilizing 8-oxoG in clinical treatment to skeletal muscle damage-related disorders.

1. Introduction

Skeletal muscle remodeling is essential for the maintenance of muscle homeostasis and physical performance. In mouse and human, the muscle-remodeling response begins rapidly upon physical exercise, which generates ROS [1,2], and mitochondria are one of the primary sources of ROS during skeletal muscle contraction. Physical exercise-resulted ROS oxidize proteins, lipids and nucleic acids; however, ROS have been regarded beneficial for muscle adaptation, including increased angiogenesis, elevated mitochondrial biogenesis and oxidative redox balance [3,4]. Exercise-produced metabolites such as xenobiotics, peptides, nucleotides, lipids, amino acids, cofactors and vitamins, carbohydrates have been recognized to act as signaling molecules [5]. However, how exercise-induced DNA oxidative damage as well as the repair metabolites impact muscle remodeling in response to exercise is poorly understood.

* Corresponding author. The Key Laboratory of Molecular Epigenetics of Ministry of Education, Northeast Normal University, Changchun, Jilin, 130024, China.
E-mail address: baxq755@nenu.edu.cn (X. Ba).

https://doi.org/10.1016/j.redox.2023.102634
Received 6 January 2023; Received in revised form 3 February 2023; Accepted 10 February 2023
Available online 15 February 2023

In general, ROS participate in oxidative assaults to DNA, producing oxidized bases, oxidized sugar fragments, apurinic/apyrimidinic (AP) sites and strand breaks. DNA lesions should be repaired per the genome integrity and fidelity ought to be maintained. Among these damages, base oxidation is predominant, 8-oxo-7,8-dihydroguanine (8-oxoguanine, 8-oxoG) is one of the most frequent DNA base lesions due to guanine's lowest redox potential out of four bases [6], and it is repaired by OGG1-initiated base excision repair (BER) in mammalian cells [7]. The excised free 8-oxoG in various human body fluids (plasma, saliva, urine as well as cerebrospinal fluid) are detectable and has been taken as the biomarker of oxidative stress [8,9].

The remodeling of skeletal muscle is dependent on myogenic specific precursor cells, referred to as satellite cells (SCs) [10]. In adult skeletal muscle, SCs are located between the sarcolemma and basal lamina, and exist in a quiescent state [10]. Once activated, SCs proliferate and differentiate, contributing to the repair of existing muscle fibers through the formation of new myonuclei, a process known as myogenesis. Extracellular components in the satellite cell niche regulate SCs fate [11], and the roles of extrinsic factors in the local microenvironment in muscle remodeling have received increasing attention [12]. Especially, redox-sensitive cues (such as cytokines, immune cells, signaling molecules) emerging from the surrounding microenvironment have been taken as crucial factors for SCs activation [13].

Studies showed that after exercise, OGG1 level/activity in muscle is increased [14,15], which implies a generation of exercise-induced DNA oxidative damage and the necessity of removal of 8-oxoG; however, whether myofiber-released 8-oxoG base functions as a signal molecule in SC niche, and is exploited to regulate myogenesis and muscle remodeling has not been understood. 8-OxoG base, the repair metabolite of the oxidized guanine lesion, has long been taken as a dull waste to be excreted, until recently, OGG1·8-oxoG complex was demonstrated to function as a guanine-nucleotide exchange factor (GEF), inducing activation of Ras and Rho GTPases [16,17]. Herein, we speculate that exercise induces 8-oxoG generation in myofiber, and after excised and

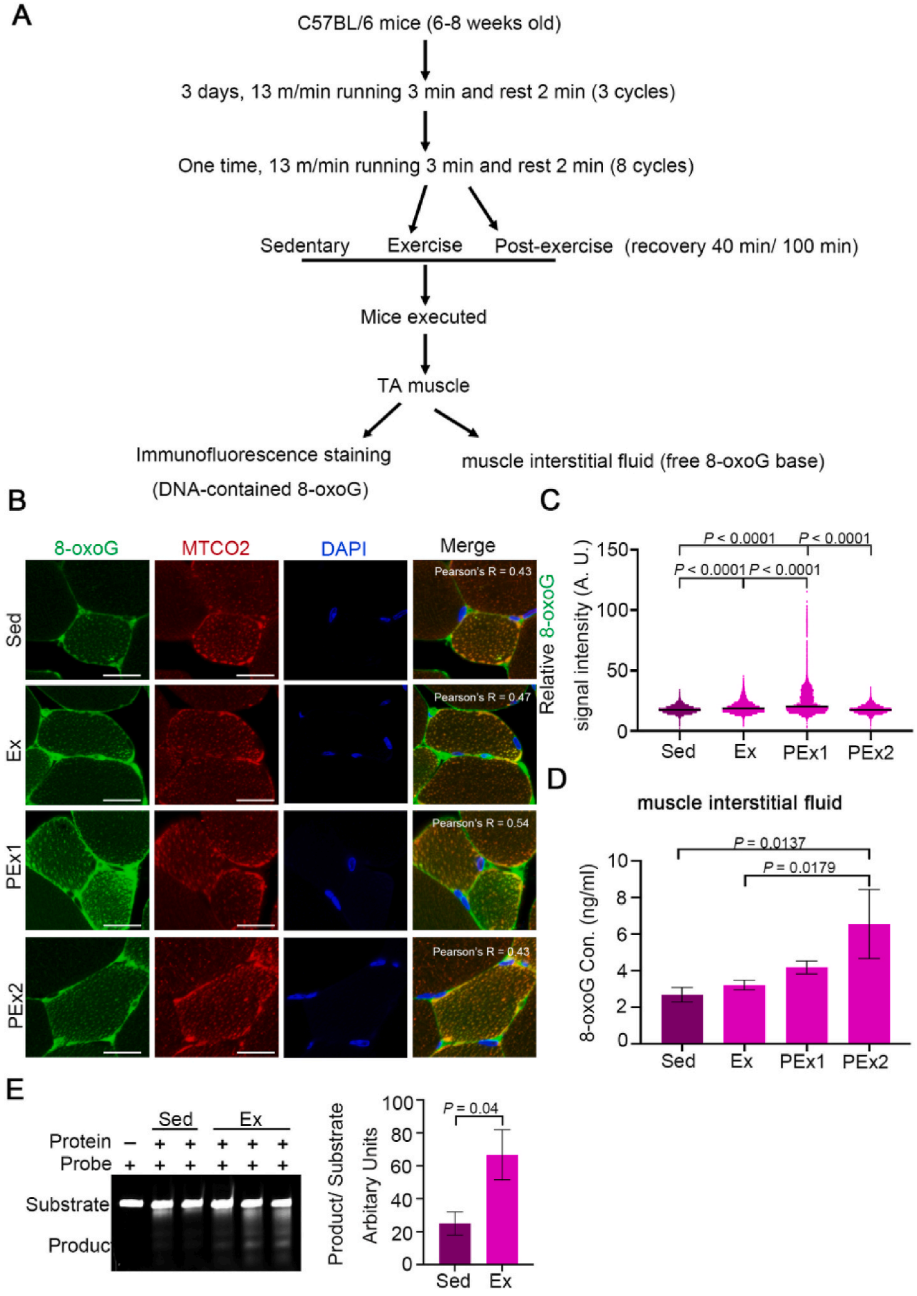

Fig. 1. Exercise induces 8-oxoG generation in mitochondrial DNA, which is gradually released in pace with rest.

A. Schematic diagram shows experimental design for the mice exercise process and sample management. Mice were randomly divided into 4 groups: 1) without exercise (basal), 2) exercise for 40 min, 3) exercise for 40 min and then rest for 40 min, and 4) exercise for 40 min and then rest for 100 min. The exercise procedure is designed as illustrated.

B. Exercise increases the level of 8-oxoG in mitochondria. Representative images of tibialis anterior (TA) cross-sections of mice differently treated as described above were co-stained with MTCO2 (red), 8-oxoG (green), and DAPI (blue), and are shown at magnification of × 63 oil objective. Signal intensity of 8-oxoG was measured. The statistical significance was determined by one-way ANOVA and sidak's post hoc testing. Scale bar, 100 μm. (mice, n = 3).

C. Quantitative analysis of the 8-oxoG levels shown by TA muscle IF staining data from (B).

D. 8-OxoG metabolite contents in interstitial fluid of TA muscles from differently treated mice. Mice were treated as described in legend **A**, interstitial fluid of TA muscles was collected and the mass spectrometry analysis was conducted as described in Method (each group, n = 20).

E. Exercise increases the catalytic activation of Ogg1 in TA muscle. 8-OxoG-containing probe cleavage assay was conducted by using the TA homogenates (10 μg) from sedentary and exercised mice. Shown are representative images from three independent experiments (Left); Quantitative analysis of the ratio of product/substrate was performed (Right). The statistical significance was determined by student's *t*-test (two-tailed, unpaired). (For interpretation of the references to color in this figure legend, the reader is referred to the Web version of this article.)

released into SC niche, 8-oxoG base enters the activated SCs, triggering Ras activation, and thereby, augmenting the expression of myogenic regulatory factors and the force producing targets.

2. Results

2.1. Exercise induces guanine oxidation in mitochondrial DNA in TA muscle and the release of repair product 8-oxoG

Acute exercise intervention is known to initiate muscle remodeling and provide systemic health benefits [1,18]. To test our hypothesis, first, we utilized a well-documented single bout of animal exercise model with slight modification as described in Methods [19]. Briefly, after 3 days of familiarity with the treadmill, mice were subjected to exercise for one time (Fig. 1A). Following exercise, mice were immediately sacrificed or allowed to recover for 40 min or 100 min. Thereafter, the tibialis anterior (TA) muscle, the major muscle engaged in treadmill running [20] was rapidly isolated. The tissues were immediately fixed for immunostaining of 8-oxoG, or subjected to centrifuge for interstitial muscle fluid collection (Fig. 1A).

An anti-8-oxoG antibody that specifically recognizes 8-oxoG in DNA duplex was used to perform immunofluorescence microscopy with the cross sections of TA muscles. Counter-staining of nucleus and mitochondrial MTCO2 revealed that 8-oxoG signals were well co-localized with subsarcolemmal and intermyofibrillar mitochondria, indicating that 8-oxoG was mainly accumulated in mitochondrial DNA (Fig. 1B). While the sedentary mice bore a certain level of 8-oxoG, exercise significantly induced the increase in 8-oxoG content in exercised mice myofibers, that reached the maximum at 40 min post exercise and then reduced at 100 min (Fig. 1B and C). We also noticed that 8-oxoG-generation was related to the type of myofibers that have more mitochondria content, the typical characteristic of the slow-twitch muscle fibers. Next, mass spectrometry was performed to determine the level of free 8-oxoG base in metabolites locally secreted from exercising muscle as described in Methods. Interstitial fluid samples were rapidly collected from TA muscles of differently treated mice. Compared with that from the sedentary mice, the amount of 8-oxoG base in the muscle interstitial fluid of the mice immediately sacrificed after exercise did not significantly increase. However, when the mice were allowed to have a rest, the amount of 8-oxoG base in the muscle interstitial fluid gradually increased. Concentrations of 8-oxoG were 2.65 ng/ml (15.8 nM), 3.3 ng/ml (19.76 nM), 4.24 ng/ml (25.44 nM) and 6.55 ng/ml (39.19 nM) respectively for sedentary, exercised, 40-min and 100-min rested mice. The concentration of 8-oxoG in interstitial fluid of the mice having a 100-min rest after exercise was about 2 folds higher compared with that of the sedentary mice (Fig. 1D). To further confirm the exercise-induced catalytic activation of Ogg1 in TA muscle, 8-oxoG-containing probe cleavage assay was conducted, result showed TA homogenates from the exercised mice possessed higher capacity to cleave 8-oxoG-containing probe, compared with that of the sedentary mice (Fig. 1E). Taken together, data indicated the local release of 8-oxoG by TA muscle is a rapid response to exercise, suggesting the DNA damage metabolite 8-oxoG is a local extracellular metabolite signature of acute exercise.

2.2. 8-OxoG elicits a global expression of myogensis-promoting genes

To test whether DNA repair metabolite 8-oxoG originated from exercised muscle could be essential for myogenesis that controls muscle remodeling, the immortalized C2C12 myoblasts were first utilized to mimic SCs differentiation (Supplementary Figs. 1A–1B). To induce C2C12 differentiation, cell culture was shifted into differentiation medium, and the expression of *MyoD*, *M-cadherin* and *Myogenin* was determined. The expression of *MyoD* and *M-cadherin* reached the maximum level at day 3, and that of *Myogenin* peaked at day 4 (Supplementary Fig. 1C). Thus, day 4 in DM was chosen to investigate whether 8-oxoG plays role in myogenic differentiation. According to the concentration applied in the previous studies [21], cells were exposed to 10 μM of 8-oxoG (guanine base (G) used as a control). Addition of 8-oxoG but not G significantly increased *Myogenin* expression at 30 min (Fig. 2A). This rapid response was consistently observed although the level of the increase in *Myogenin* expression was not robust. To test a cumulative effect of the exposure that might suit a long-term exercise scenario, 8-oxoG was successively administrated from day 3 to day 5, and MHC, the functional target of Myogenin, was detected. The result showed a significant increases in number of MHC positive cells as well as fused myotubes. Immunofluorescence assay revealed that MHC mainly accumulated in the multiple-nuclear myotubes (Fig. 2B). The fusion index of 8-oxoG-treated C2C12 cells, but not that of control cells treated with guanine, was significantly increased (Fig. 2C). A gradual increase in MHC expression in response to 8-oxoG addition was verified by western-blotting (Fig. 2D).

To further address the myogensis-promoting role of 8-oxoG in a global view, RNA sequencing (RNA-seq) was performed to interrogate the transcriptomic changes caused by 8-oxoG exposure (from day 3 to day 5). We found 937 differentially expressed genes (DEGs) between vehicle- and 8-oxoG-treated cells, among them, 460 up-regulated and 477 down-regulated. The volcano plot showed the distribution of differentially expressed genes between vehicle- and 8-oxoG-treated cells (Fig. 3A). The representative genes with high significance are highly relevant to myoblast differentiation (such as Myog, Mef2c), and associated with skeletal muscle functions (such as Tnni2, Myh1, Myh7 and Myh8) (Fig. 3A). According to GO analysis, up-regulated genes in 8-oxoG-treated cells were enriched in biological processes related to muscle contraction, muscle cell development, and muscle organ development. This result revealed the activation of development processes in muscle cells in response to 8-oxoG treatment (Fig. 3B and Supplementary Figs. 2A–2B). Moreover, according to the KEGG enrichment analysis, 8-oxoG-induced pathways are highly related to the focal adhesion, including pathways regulating hypertrophic cardiomyopathy, regulation of actin cytoskeleton pathways (Fig. 3C). Taken together, data of RNA-Seq not only verified the role of 8-oxoG in *Myogenin* expression revealed by RT-qPCR, also suggested that exercise-generated 8-oxoG metabolite can be regard as a signal entity, globally promoting the myogenic differentiation of myoblasts.

2.3. 8-OxoG enhances transcriptional activity of MyoD in myoblasts

During myoblasts differentiation, transcription factor Myogenin is the target of MyoD, and is an irreversible differentiation marker of skeletal muscle [22]. We hypothesized that 8-oxoG-triggered signaling may facilitate MyoD transcriptional programs. To this end, chromatin immunoprecipitation (ChIP) assay was conducted using C2C12 cells. The result showed a significant increase (~3.6 folds) in the association of MyoD with *Myogenin* promoter in response to 8-oxoG treatment (the immunoglobulin heavy locus (IgH) served as negative control). An enhanced binding of MyoD was also observed with promoters of *M-cadherin, MHCIIb* and *muscle creatine kinase* (*MCK*) (2.0, 1.6 and 3.8 folds, respectively), as well as *MCK* enhancer (2.8 folds) (Fig. 4A–F). To validate these results, we performed the *Myogenin* promoter-driven Luciferase (Luc) dual reporter assays using MyoD-overexpressing C3H10T1/2 fibroblasts. Luc activity assay showed 8-oxoG exposure-induced increase in *Myogenin* promoter activation compared with that of control (Supplementary Fig. 3A). Likewise, the mRNA level of firefly luciferase showed >2.5-fold increase in cells exposed to 8-oxoG for 30 min (Fig. 4G).

To further affirm that 8-oxoG exposure could enhance MyoD binding with its consensus motif, EMSA assays were conducted using MCK promoter-derived MyoD site-containing probe [23]. First, recombinant protein GST-MyoD, but not GST shifted MCK promoter-derived probe in a dose-dependent manner (Supplementary Fig. 3B), which could be diminished by MyoD site mutation (Supplementary Fig. 3B) or competed out by excess cold probe (Supplementary Fig. 3C), validating the probe

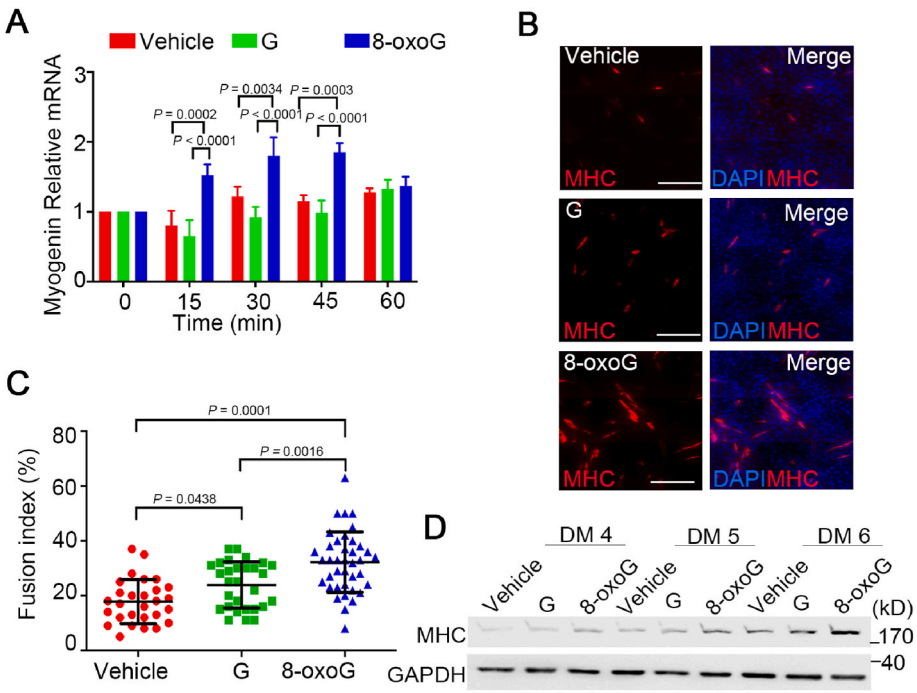

Fig. 2. 8-OxoG increases the expression of differentiation markers in C2C12 myoblasts.

A. Exposure of 8-oxoG augments expression of *Myogenin*. Cells at day 4 in DM were exposed to 8-oxoG or guanine (G) at 10 μM, or mock-treated for different time lengths (0, 15, 30, 45 and 60 min). Then, RT-qPCR analysis of mRNA level of *Myogenin* was carried out. Two-way ANOVA and Tukey's post hoc testing was used to calculate the statistical significance.

B-D. Exposure of 8-oxoG accelerates myogenic differentiation. C2C12 myoblasts in DM were successively exposed to 8-oxoG (10 μM) or controls from day 3 to day 5 (once a day), immunofluorescence staining was conducted at Day 6 to show the expression of differentiation marker MHC (red), nuclei were counterstained with DAPI (blue). Scale bar: 100 μm. Shown are the representative images from three independent experiments (**B**). MHC^{+} cells were counted and presented as fusion index. One-way ANOVA and Tukey's post hoc testing was used to calculate the statistical significance (**C**). Every second day after 8-oxoG exposure, total cell lysates were prepared and resolved in 10% SDS-PAGE. Western-blotting was conducted to assess the protein level of MHC, and the expression of GAPDH was taken as internal control. Shown are the representative images from three independent experiments. The band intensity was quantified by using the Image J software (1.43 V, US National Institutes of Health). The value of the band density for vehicle-treated group was taken as 1 (**D**). (For interpretation of the references to color in this figure legend, the reader is referred to the Web version of this article.)

as the substrate of MyoD. Next, nuclear extracts (NE) from vehicle-, guanine-, or 8-oxoG-treated cells were subjected to EMSA. Result showed that 8-oxoG treatment increased the amount of protein-probe complex (Fig. 4H). To verify the involvement of MyoD in the formation of the DNA-protein complex, we interfered the expression of MyoD since the super-shift assay did not work, and the result showed the complex amount was reduced if MyoD was knock-down. (Fig. 4I). Moreover, to confirm the existence of MyoD in the protein-probe complex, we performed probe pull-down assay. C3H10T1/2 fibroblasts were transfected with GFP-MyoD, and then exposed to 8-oxoG for 0, 10, 20, 30 min, and the nuclear extracts were prepared. The result showed that MCK promoter-derived probe-bound GFP-MyoD gradually increased, and reached to ~2 folds if the NE was made from cells with 30-min 8-oxoG exposure (Supplementary Fig. 3D); whereas, src promoter-derived probe only merely bound with GFP-MyoD (Supplementary Fig. 3E).

Previous studies showed that phosphorylation of MyoD at tyrosine (Y) 156 promoted the functions of MyoD in muscle differentiation [24]. To verify the role of 8-oxoG in the enhancement of the transcription activity of MyoD, tyrosine phosphorylation were detected. Western-blotting analysis showed in response to 8-oxoG treatment, the phospho-Tyr-MyoD protein level increased from 5 min on, reached the maximum (more than 3 folds) by 10 min, and then decreased to the basal level at 20 min (Fig. 4J). To address whether tyrosine phosphorylation of MyoD attribute to the increase in the transcriptional activity, wild type (WT) and Y156F/V site mutated MyoD were overexpressed in C3H10T1/2 fibroblasts, and the cells were exposed to 8-oxoG, luciferase dual reporter assays were performed. The mRNA level of firefly luciferase was increased >1.6-fold in WT MyoD-expressing cells, which was not observed in Y156F or Y156V mutated MyoD-expressing cells (Fig. 4K). Increase in the mRNA level of firefly luciferase induced by 8-oxoG administration was retreated if the binding site of MyoD in *Myogenin* promoter was mutated (Fig. 4L). Taken together, these data indicated that 8-oxoG promote myoblasts differentiation through enhancing the transcriptional program triggered by MyoD.

2.4. Activation of Ras-MEK-MyoD signaling axis by 8-oxoG

Findings over the past years have unambiguously established the key roles of MAPK pathways in regulation of myogenic program at multiple stages [24,25]. Thus, we examined the phosphorylation levels of ERK1/2, p38 and JNK in C2C12 cells exposed to 8-oxoG. Intriguingly, all these three MAPKs displayed a significant increase in the levels of phosphorylation although the time kinetics was different. Within 30 min, ERK1/2 and JNK exhibited a pulse of phosphorylation at 15 min; whereas, p38 phosphorylation manifested a bi-phase pattern in that a 10-min peak was followed by a relatively higher apex shown on 30 min (Fig. 5A). Nevertheless, EKR1/2 kinase (MEK1/2) inhibitor U0126 markedly blocked 8-oxoG-induced MyoD phosphorylation (Fig. 5B). Accordingly, 8-oxoG exposure-induced ERK1/2 phosphorylation was reduced nearly to basal level by U0126 (Fig. 5C). Importantly, pharmacological inhibition of ERK but not JNK and p38 kinase significantly suppressed expression of *Myogenin* mRNA (Fig. 5D).

Activation of small GTPases is the upstream signaling event of MAPK pathway. Thus, we performed active Ras, Rac1/Cdc42 and RhoA pull-down assay. At day 3 of differentiation, the C2C12 cells were challenged with 8-oxoG, and the lysates were prepared from cells with 0-, 3-, 6-, 9-, 12-min 8-oxoG exposure. While a rapid and robust increase in the Ras-GTP level was observed (~3 min), levels of RhoA-GTP and Rac1-GTP were also increased at a later phase, but activated Cdc42 was not detectable (Fig. 5E–H). Inhibitors of Rac1/Cdc42 and RhoA were applied while C2C12 cells were exposed to 8-oxoG. Western-blotting showed that ERK1/2 phosphorylation was not reduced under these conditions (Fig. 5I). However, Ras inhibitor caused a marked decrease in the phosphorylation of the ERK1/2 (Fig. 5J), suggesting an activation of MEK1/2 through RasGTPase in 8-oxoG-exposed myoblasts. Collectively, data strongly support that 8-oxoG function as a signal molecule, triggering Ras-MEK-MyoD axis activation, promoting myogenic

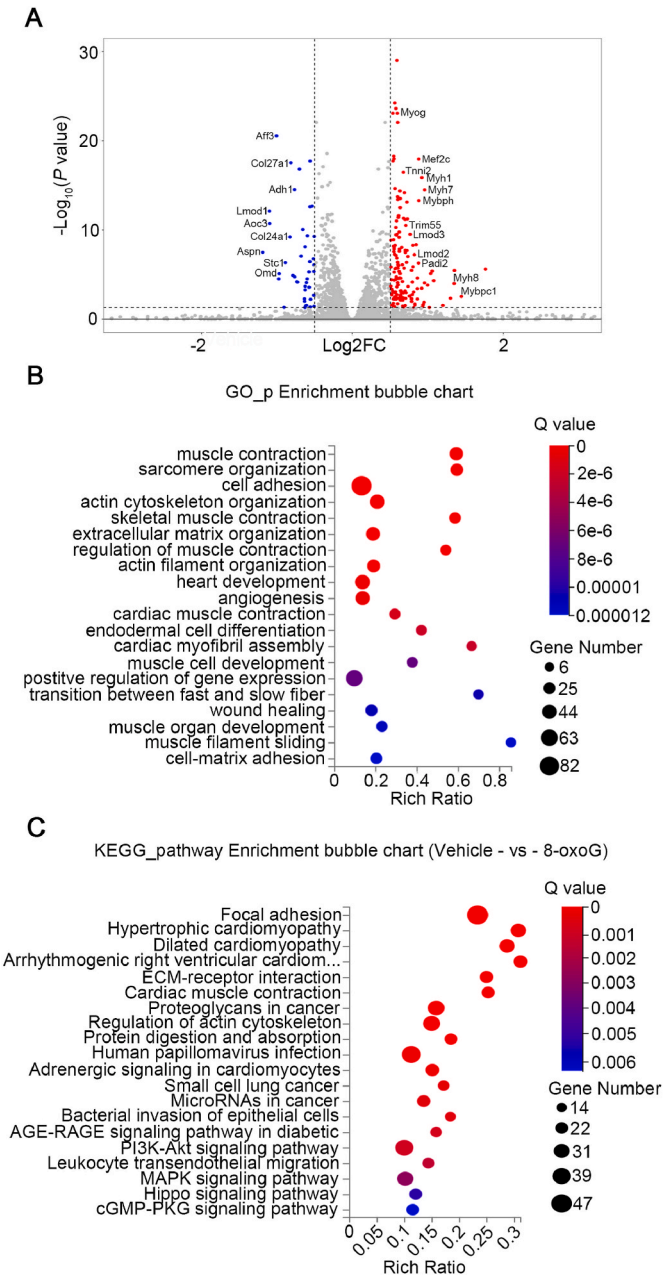

Fig. 3. RNA sequencing (RNA-seq) analysis identifies the gene expression profile regulated by 8-oxoG. C2C12 myoblasts in DM were successively exposed to 8-oxoG (10 μM) or vehicle from day 3 to day 5 (once a day), at Day 6, RNAs were exrtacted, RNA-seq was conducted.

A. Volcano plot showing distribution of differentially expressed genes between vehicle and 8-oxoG treatment cells. Adjusted p value < 0.05. The color scheme with upregulation in red, downregulation in blue, and undetermined directionality in gray.

B. Gene ontology (GO) term enrichment analysis for genes that are differentially expressed between vehicle and 8-oxoG C2C12 cells.

C. KEGG enrichment analysis presented several pathways highly related to stem cell traits compare vehicle to 8-oxoG. (For interpretation of the references to color in this figure legend, the reader is referred to the Web version of this article.)

differentiation of myoblasts.

2.5. OGG1 is required for the signaling role of 8-oxoG in myogenic differentiation

8-OxoG functions as a signal ligand, which raises a question as to what could be its cognate recognizing/binding protein to mediate the activation of Ras-MEK-MyoD pathway. Studies have substantially documented that the repair enzyme OGG1 forming complex with the excised free 8-oxoG base with high affinity, functions as a GEF, triggering downstream cellular signaling via the Ras and Ras homology family GTPases [16,17]. To investigate whether OGG1 affects myoblasts differentiation, Ogg1 expression in C2C12 cells was depleted by siRNA. Silencing Mth1 was taken as the control. The efficiency of siRNA interference were confirmed (Supplementary Fig. 4A), and then, the expression of *Myogenin* in cells with 8-oxoG exposure was assessed. Results showed that 8-oxoG-induced increase in expression of *Myogenin* was significantly eliminated by Ogg1 silencing, whereas, si-Mth1 had a negligible effect (Fig. 6A). EMSA analysis further confirmed the decrease in probe binding of MyoD from the 8-oxoG-treated Ogg1 knocked down cells, whereas the Mth1-interfered cells only displayed a slight impairment (Fig. 6B). Moreover, Ras activity was tested, and the result showed that compare to si-Mth1 and non-targeting si-control, si-Ogg1 markedly decreased the level of active Ras (Fig. 6C).

To determine the affinity and the specificity of OGG1 forming a complex with 8-oxoG, the established MST assay was utilized. As expected, association of OGG1 with guanine was not detectable, whereas, the dissociation constant (*Kd*) values of OGG1 with 8-oxoG and 8-hydroxyguanosine were 0.7 ± 0.33 nM and 2.01 ± 0.31 nM, respectively (Fig. 6D–F). In controls, the interaction of MTH1 with 8-oxoG was also examined, and the *Kd* value was about 1.5 fold higher than that of OGG1 (Supplementary Figs. 4B–4C). Taken together, these results suggest that OGG1 bind with 8-oxoG and mediate Ras-MEK-MyoD activation in myogenic differentiation.

2.6. 8-OxoG-triggered signaling is impaired in Ogg1 knockout mice

To further validate the role of OGG1 in muscle remodeling, *Ogg1* knock-out (KO) mice were utilized in exercise. First, WT and *Ogg1* KO mice were subjected to a 7-day exercise, and after the last bout of running (40 min), the TA muscles were collected, and the 8-oxoG localization as well as the expression of *MyoD* and *Myogenin* was measured. Immunofluorescence staining of the cross sections of TA muscles showed that the sedentary *Ogg1* KO mice bore higher level of 8-oxoG accumulated in TA mitochondria than WT mice, reflecting a defect in Ogg1-initiated lesion excision. Nevertheless, exercise increased the amount of 8-oxoG in TA muscle of both WT and *Ogg1* KO mice, and typically of the latter ones (Fig. 7A and B). Next, gene expression was measured. Compared with that of sedentary group, exercise only induced a significant increase in *Myogenin* mRNA level in WT mice (p = 0.027) but not in *Ogg1* KO mice; whereas, MyoD transcription did not exhibit significant alterations in response to exercise in both WT and KO mice. Among those exercised mice, both *MyoD* and *Myogenin* mRNA levels from *Ogg1* KO mice were significantly lower than that from WT mice (p values were 0.0026 and 0.0071 respectively), however, the *Ogg1* depletion-imposed impairment to the exercise-induced increase in *Myogenin* expression was more significant than that of *MyoD* (p values were 0.0253 vs 0.0415) (Fig. 7C and D). These results were in line with increased Ras activation and ERK phosphorylation in SCs isolated from exercised WT but not *Ogg1* KO mice (Fig. 7E and F).

To confirm the importance of OGG1 in mediating signaling role of 8-oxoG base, an *ex vivo* assay was set up by utilizing isolated SCs as described previously [26]. Primary SCs were kept in proliferation medium for 6 days and then shifted to differentiation medium (DM). SCs' morphological change was recorded, and MyoD immunofluorescence staining was performed at day 3 of differentiation to identify the

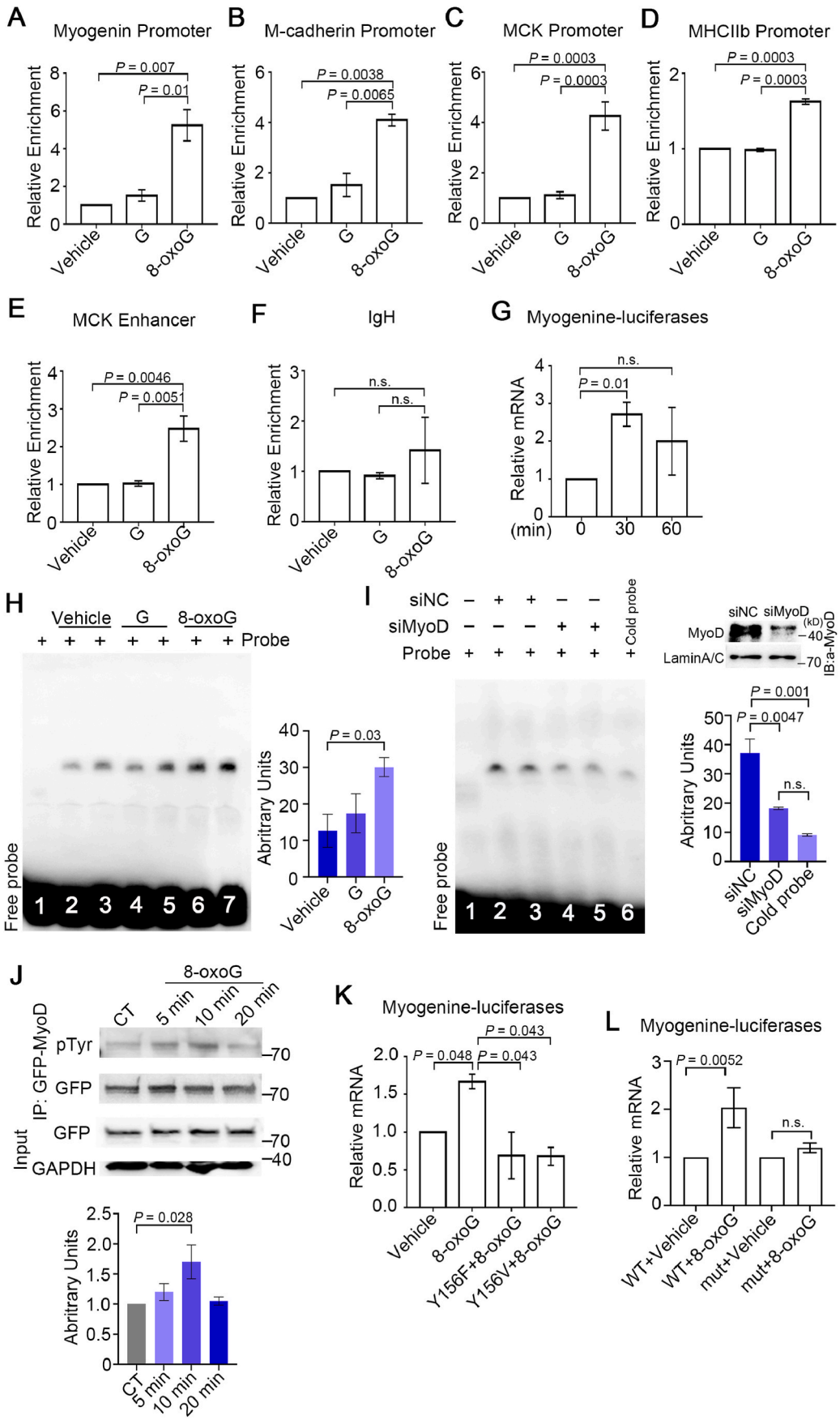

Fig. 4. 8-OxoG promotes transcriptional activity of MyoD.

A-F. Increased accumulation of MyoD on regulatory regions of targets in response to 8-oxoG exposure. C2C12 myoblasts were challenged with 8-oxoG or guanine (G) in DM for 4 days (once a day). At 30 min after the last challenge, ChIP-qPCR was conducted by using an antibody against MyoD to analyze the presence of the protein at the regulatory regions of 6 representative myogenic genes and the negative control immunoglobulin heavy locus (IgH). One-way ANOVA and Tukey's post hoc testing was used to calculate the statistical significance.

G. 8-OxoG activates transcription of *Myogenin* by MyoD. C3H10T1/2 cells were transfected with *Myogenin* promoter-driven Luciferase dual reporter system along with Flag-tagged MyoD expressional plasmid. Cells were 8-oxoG-treated 30 or 60 min and after exposure, RNAs were exacted, levels of firefly luciferase mRNA that presents *Myogenin* promoter activation were assessed by taking levels of Renilla mRNA as internal controls. One-way ANOVA and Tukey's post hoc testing was used to calculate the statistical significance.

H–I. 8-OxoG exposure enhances MyoD binding with target sequence. Nuclear extracts (NEs) from C2C12 cells treated with 8-oxoG or G, or mock-treated for 30 min at day 4 of differentiation were prepared, and EMSA was conducted (**H**). The specificity of MyoD in the protein-DNA complex was determined by small RNA knock-down of MyoD and cold probe competition, and the efficacy of MyoD interference was provided at right upper panel (**I**). Shown are the representative images from three independent experiments, and quantitative analysis of the density of protein-DNA complex was shown at the right panels.

J-L. Phosphorylation of Y156 accounts for 8-oxoG-induced transcriptional activation of MyoD. C3H10T1/2 cells were transfected with GFP-MyoD, and then exposed to 8-oxoG for 5, 10, 20 min. Tyrosine phosphorylation of MyoD was tested by immunoprecipetation of GFP-tagged protein flowed by western-blotting. Shown is the representative image from three independent experiments, and quantitative analysis of the density of protein was shown at the lower panel (**J**). C3H10T1/2 cells were transfected with *Myogenin* promoter-driven Luciferase dual reporter system along with plasmids expressing GFP-tagged wild-type MyoD or Y156F/V mutants. Cells were exposed to 8-oxoG for 30 min, RNAs exacted, levels of firefly luciferase mRNA assessed by taking levels of Renilla mRNA as internal controls. One-way ANOVA and

Tukey's post hoc testing was used to calculate the statistical significance (**K**). The binding site of MyoD in *Myogenin* promoter was mutated. C3H10T1/2 cells were transfected with the WT and mutant Luciferase dual reporter system along with Flag-tagged MyoD expressional plasmid. Promoter activity analysis was conducted as described in (**L**).

myogenic precursors (Supplementary Fig. 5A). The result showed that >95% of cultured cells were MyoD-positive (Supplementary Fig. 5B). First, the SCs from WT mice were used to measure the time dynamic of gene expression (Fig. 8A). The result showed that the expression of *Myogenin* reached the maximum level at day 6 in differentiation medium. To determine the direct effect of 8-oxoG on myoblasts differentiation, cells were exposed to 8-oxoG at day 6 in DM. The result showed an increase in the expression of *Myogenin* in myoblasts from WT but not *Ogg1* KO mice (Fig. 8B).

To further assess the impact of 8-oxoG on cell differentiation, myoblasts in DM were successively exposed to 8-oxoG or vehicle from day 3 to day 6, and MHC^{+} cells were detected. Immunofluorescence staining revealed that deletion of *Ogg1* reduced the increase in myotube fusion shown by MHC^{+} cells (Fig. 8C and D). To determine the downstream signaling of ERK, myoblasts in DM at day 6 were treated with 8-oxoG for 15 min (Fig. 8E). The result showed that the addition of 8-oxoG induced rapid increase in the phosphorylation ERK in myoblasts. Whereas, the phosphorylation of ERK is slight increase in primary myoblasts isolated from *Ogg1* KO mice. Moreover, Ras inhibitor treatment weakened the phosphorylation of ERK, indicating Ras is involved in the process (Fig. 8E). These *ex vivo* assays indicated that OGG1 is essential for the role of 8-oxoG in activation of Ras-ERK signal axis and expression of myogenic factors.

2.7. Exogenously administrated 8-oxoG base may promote the regeneration of injured muscle

The signaling effect of 8-oxoG during exercise urged us to further explore the therapeutic potential of 8-oxoG administration in muscle regeneration after injury. TA muscle of mouse was injured by injection with the snake venom cardiotoxin (CTX) as described [27], and TA were collected at 1, 3, 5, 7, 9 and 11 days. The expression of *MyoD* and *Myogenin* was analyzed by RT-PCR to evaluate the regeneration after CTX injection (Supplementary Fig. 6A-6B), and the expression of *MyoD* and *Myogenin* showed the peak at day 3 (2.86 ± 1.63 folds and 24.4 ± 2.14 folds, respectively). The CTX injection did not cause significant alteration in body weight (Supplementary Fig. 6C). Accordingly, 8-oxoG was administered intramuscularly (saline injection as control) (Supplementary Fig. 6D), and day 3 and day 7 were chosen to examine the effect of 8-oxoG administration. First, the histological analysis indicated that without muscle injury, there was no significant difference observed between TA muscles with saline or 8-oxoG injection (Supplementary Fig. 6E). And then the expression of *MyoD* and *Myogenin* of TA muscles during recovery was examined. The results showed that the 8-oxoG promoted the expression of *MyoD* at day 3 and *Myogenin* at day 7 post CTX injection (Fig. 9A and B). Importantly, 8-oxoG administration did not show effect on expression of myogenic factors in *Ogg1* KO mice (Fig. 9C and D). Next, we assessed the effect of 8-oxoG treatment on muscle recovery at 7 day after CTX damage. In WT mice, the size of regenerated myofibers (eMyHC-positive myofiber) were larger in size in 8-oxoG-injected TA muscle compared to that of saline-treated ones (Fig. 9E–G). We did not observe the marked discrepancy between the morphology and the weight of TA muscles treated with 8-oxoG and saline in *Ogg1* KO mice (Fig. 9E–G), in line with the result of gene expression measurement (Fig. 9C and D). Collectively, data confirmed that 8-oxoG injection lead to an acceleration of recovery of injured muscle, supporting a potential significance of 8-oxoG to a therapeutic scope.

3. Discussion

Skeletal muscle has been considered as an endocrine organ, and the muscle fibers secrete various factors [28], providing an immediate niche for the SCs, which are located between the sarcolemma and the basal lamina of muscle fibers. Satellite cell functions can be improved by both resistance and endurance exercise [29]. Exercise increase ROS concentration in skeletal muscle, that inevitably modify bio-macromolecules including DNA in myofibers. ROS have been regarded as beneficial for muscle adaptation and regeneration [3,30,31]. However, whether repair metabolites of oxidatively damaged DNA play roles in modulating SCs functions is elusive. Our present study posted an unexpected role of 8-oxoG base, the repair product of oxidized guanine from DNA, in myogenesis. After released from myofiber, 8-oxoG is engaged with OGG1 in the activated SCs, promotes myoblast differentiation via evoking Ras-MEK signaling pathway and enhancing MyoD transcriptional program (Figs. 2–5, Fig. 10). Thus, the present study revealed that DNA metabolites of myofiber can provide *in situ* niche signaling to regulate stem cell functions, providing a new perspective to understand the benefits of exercise-generated ROS.

Mitochondria are one of the major sources of ROS production; thus the mitochondrial DNA (mtDNA) contained therein are particularly prone to being affected by oxidative insults. In the present study, an increase in 8-oxoG in myofiber mitochondria in response to exercise was observed (Fig. 1A–D). The kinetic changes of 8-oxoG level in myofiber mitochondria suggested a generation of mitochondria-sourced 8-oxodG and a liberation of 8-oxoG from mitochondrial genome by mitochondrion-located Ogg1. Intriguingly, previous study documented that exercise improves import of Ogg1 into the mitochondrial matrix of skeletal muscle and enhances its relative activity [15], which signifies the release of the repair product. In line with the previous observation, the present study revealed that 8-oxoG excision activity of the TA muscle from exercised mice significantly increased (Fig. 1D). The excised free 8-oxoG in various human body fluids (plasma, saliva, urine as well as cerebrospinal fluid) has been detected and taken as the biomarker of oxidative stress [32]. In the present study, metabolite mass spectrometry assay validated a significant increase in 8-oxoG content in the interstitial fluid from TA muscle of the mice that have a 100 min rest post exercise, supporting a consequence that 8-oxoG is released from myofiber into the niche of SCs. Uptake of 8-oxoG is speculated through transporter ENT2 that is involved in transporting the nucleosides and nucleobases of purine and pyrimidine molecules [33]. Intriguingly, expression of ENT2 is mostly abundant in skeletal muscle among various types of tissues [34] although the cell type-location of this transporter has not yet been determined.

A large number of studies have underlined the pivotal role of MAPK signal pathways in the growth and metabolism of skeletal muscle in response to exercise [35]. Over a given period of myogenesis, a particular kinase is activated and regulates its downstream effectors including specific myogenic transcription factors [35]. MEK and ERK1/2 have been shown to be activated at the late stage that spans from the proliferation to differentiation periods of myogenesis and involves myogenic transcription factor MyoD [24,36]. MEK1 directly phosphorylates MyoD at Tyr-156 in helix 2 of the HLH domain, allowing MyoD to escape from MAFbx/AT-1, a key E3-ubiquitin ligase necessary for MyoD degradation [24,36], increasing its stability during skeletal myogenesis. Through inducing cell cycle exit, p38 with ERK together regulates the differentiation and hypertrophic stages of myogenesis. P38 MAPK stimulates

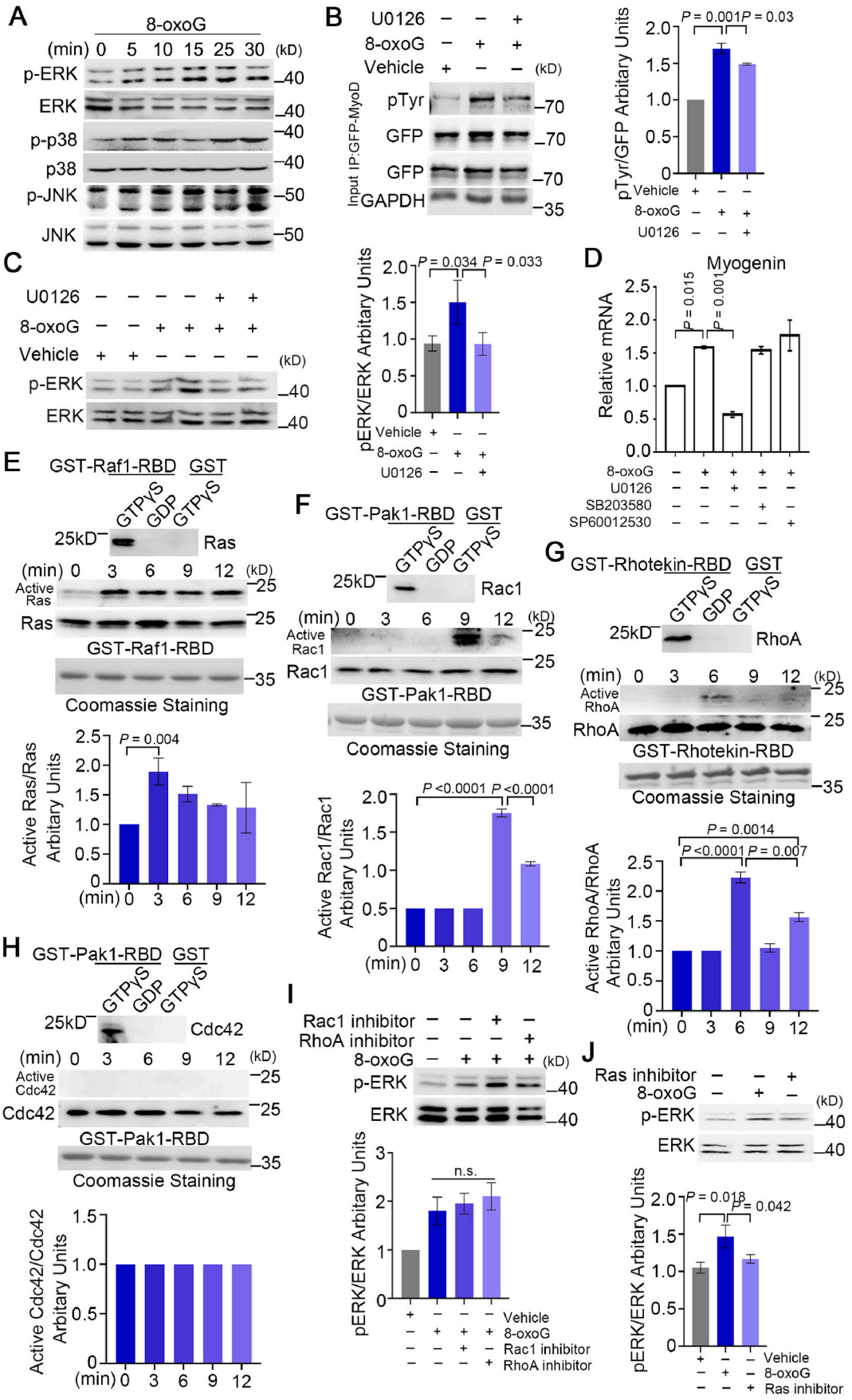

(caption on next page)

Fig. 5. 8-OxoG activates Ras-MEK-MyoD signal pathway in C2C12 myoblasts.
A. Activation of MAP kinases by 8-oxoG exposure in C2C12 cells. C2C12 cells were treated with 8-oxoG (10 μM) for 0, 5, 10, 15, 25 and 30 min and then levels of p-ERK, p-p38 and p-JNK were determined by western-blotting.
B–C. MEK activation accounts for 8-oxoG-induced tyrosine phosphorylation of MyoD. C3H10T1/2 cells were transfected with GFP-MyoD expressional plasmid and exposed to 8-oxoG (10 μM) for 10 min with or without 1-h prior treatment of MEK inhibitor U0126 (10 μM), Tyr-phosphorylation of MyoD was detected by immunoprecipitation followed by western-blotting (**B**), and the p-ERK protein levels were determined by western-blotting (Duplicates of each sample were shown) (**C**), and quantitative analysis of the density of protein was shown at the right panels.
D. Inhibition of MEK activity blocks 8-oxoG-induced upregulation of myogenin expression. C2C12 cells were pretreated with the indicated inhibitors U0126 (10 μM), SB203580 (10 μM) and SP600125 (10 μM) for 1 h in DM at day 4 of differentiation. Then the cells were exposed to 8-oxoG (10 μM) for 30 min. The mRNA level of *Myogenin* was determined by RT-PCR analysis. One-way ANOVA and Tukey's post hoc testing was used to calculate the statistical significance. **E-I. Activation of small GTPase Ras accounts for 8-oxoG-induced MEK activation.** C2C12 cells were exposed to 8-oxoG (10 μM) for 0, 3, 6, 9, 12 and 15 min in DM at day 4 of differentiation. Cell extracts were prepared and the levels of Ras-GTP (**E**), Rac1-GTP (**F**) RhoA-GTP (**G**) and Cdc42-GTP (**H**) were evaluated by the active GTPase pull-down assay as described in Methods. C2C12 cells were pretreated with Rac1 and RhoA inhibitors (**I**), and Ras inhibitor, and then exposed to 8-oxoG (10 μM) for 3 min. Phosphorylation of ERK was detected by western-blotting (**J**). Shown are the representative images from three independent experiments, and quantitative analysis of the activation of small GTPases and MEK activation were shown at the lower or right panels.

MyoD dependent gene transcription indirectly, as p38 phosphorylates MEF2 and E47 that together with MyoD form part of an active myogenic transcriptional complex [37]. JNK regulates muscle remodeling via myostatin/SMAD inhibition [38], and appears in some cases to be either dispensable or negative in myogenesis [39]. Intriguingly, in the present study, we showed that all three MAP kinase signal pathways were activated in C2C12 cells upon 8-oxoG exposure (Fig. 5A). Nevertheless, only MEK inhibitor U0126 blocked 8-oxoG-induced MyoD Tyr-156 phosphorylation and *Myogenin* transcription, while JNK inhibitor did not and p38 inhibitor slightly exhibited the reversed effect. Despite the universal activation of MAPKs and/or other potential kinases in myoblasts, which may finally be integrated into muscle remodeling in response to 8-oxoG exposure, MEK activation and tyrosine phosphorylation of MyoD present an essential molecular mechanism to support the role of 8-oxoG as a signal entity to regulate myogenic gene expression (Fig. 5A–D).

Previous studies documented that repair product 8-oxoG is engaged with OGG1. The formed complex functions as a GEF and stimulates small GTPase. In the present study, we observed a rapid, robust and persistent activation of Ras in C2C12 cells upon 8-oxoG administration (Fig. 5E). Earlier studies observed that transfection of H- or N-Ras inhibited both myoblast fusion and muscle-specific gene product expression [40]; Whereas, other study showed that the R-Ras has a positive effect on the terminal differentiation of myoblasts [41,42], implying that myogenesis depend on the difference types of Ras and downstrem signals. We also detected the activity of RhoA, Rac1 and Cdc42 GTPases. While Cdc42 did not exhibit response to 8-oxoG administration, RhoA and Rac1 displayed a pulse of activation in a later phase (Fig. 5F–H). However, RhoA and Rac1 inhibitors did not block 8-oxoG-induced MEK activation as well as MyoD Tyr phosphorylation, indicating a Ras-MEK-MyoD signaling for myogenic gene expression regulation (Fig. 5I and J). RhoA and Rac1 GTPases are well addressed to regulate cellular processes dependent on actin cytoskeleton dynamics. For instance, the RhoA/ROCK signaling pathway is crucial for contractile force generation needed for the assembly of stress fibers, focal adhesions and for tail retraction during cell migration [43]; Yet, the exact functions of these small GTPases in regulation of the reassembly of actin-based cytoskeleton in myogenesis remains largely undefined. Previous studies revealed that the presence of 8-oxoG base increases RhoA-GTP levels in cultured cells and lungs, which mediates α-smooth muscle actin polymerization into stress fibers [17]. Given the observed activation of RhoA and Rac1 that was induced by 8-oxoG (Fig. 5F–H), it is reasonable to assume that 8-oxoG may impact myogenesis or even the functions of myofiber through regulating activation of RhoA or Rac1 GTPase, subsequently modulating actin filament assembly, which needs further investigated in future.

The signaling role of 8-oxoG in myogenic differentiation as well as the contribution of Ogg1 are validated by the *in vivo* and *ex vivo* analyses. 8-OxoG accumulation in mitochondrial DNA in myofiber was enhanced by exercise, which fell back to the basal level after rest, implying repair and release of 8-oxoG (Fig. 1B–E). Given the permeation barrier property of the basal lamina that generates a unique biological niche, locally concentrated 8-oxoG, along with other exercise-induced myofiber released factors, is likely to affect the function of myogenic precursors. In the present study the expression of myogenic factor *Myogenin* as well as its functional target MHC in the primarily isolated satellite cells from WT mice, but not *Ogg1* KO ones, significantly increased in response to 8-oxoG exposure (Fig. 8C and D). In parallel, 8-oxoG addition triggered Ras signal-dependent ERK1/2 activation in primary myoblasts isolated from WT mice, but not from *Ogg1* KO ones (Fig. 8D). At the physiological level, comparison of the exercise-induced expression of myogenic factors (MyoD and Myogenin) in TA tissues from WT and *Ogg1* KO mice further affirmed the implication of OGG1 in gene expression regulation in myogenic differentiation (Fig. 7C). Accordingly, running induced an increase in ERK phosphorylation in WT mice but not *Ogg1* KO ones (Fig. 7E and F). Taking the fact that repair activity of OGG1 declines along with aging [44], we may even consider that the muscle loss in the old mice, to some extent, possibly results from the abatement of the fuel of 8-oxoG.

Based on the function of physiologically generated 8-oxoG in muscle remodeling, the therapeutic implication of exogenously administrated 8-oxoG in muscle wound healing is in expectation, and hypothesis needs further investigation in future. From tissue destruction to recovery, muscle regeneration occurs in five interrelated and time-dependent phases, namely degeneration-necrosis, inflammation, regeneration, maturation/remodeling, and functional recovery, reflecting the hierarchy of the overall process dominating the tissue [45]. At early stage, inflammation is acknowledged crucial for SCs proliferation and differentiation [45]. However, in the present study, injection of 8-oxoG alone, in absence of tissue damage, did not induce SCs activation and differentiation (Supplementary Fig. 6E), suggesting other factors (e.g. inflammatory cues) are essential for initiation of SCs activation before 8-oxoG capable to improve the healing of the injured muscle. It seems that 8-oxoG has no effect on muscle resident macrophages probably due to the difference in ENT2 expression among cell types within skeletal muscles. ENT2 has been reported highly expressed by proliferating cells and the epithelial cells of various tissues [46]. The cell-type distribution of ENT2 within skeletal muscle, as well as the expression pattern of ENT2 during myogenesis of myoblasts is an enigma to decipher in our future investigation.

4. Conclusion

In summary, our data signified that 8-oxoG base is a signaling molecule, which forms complex with OGG1 in myoblasts, orchestrating the post ROS-insult feed-back processes, promoting myogenic differentiation, and consequently, leading to skeletal muscle remodeling or adaptation. This concept not only fits physiological contexts (e.g., extensive exercise), but might also extend to pathological conditions (e.g., trauma, age-associated muscle loss), for designing strategies to

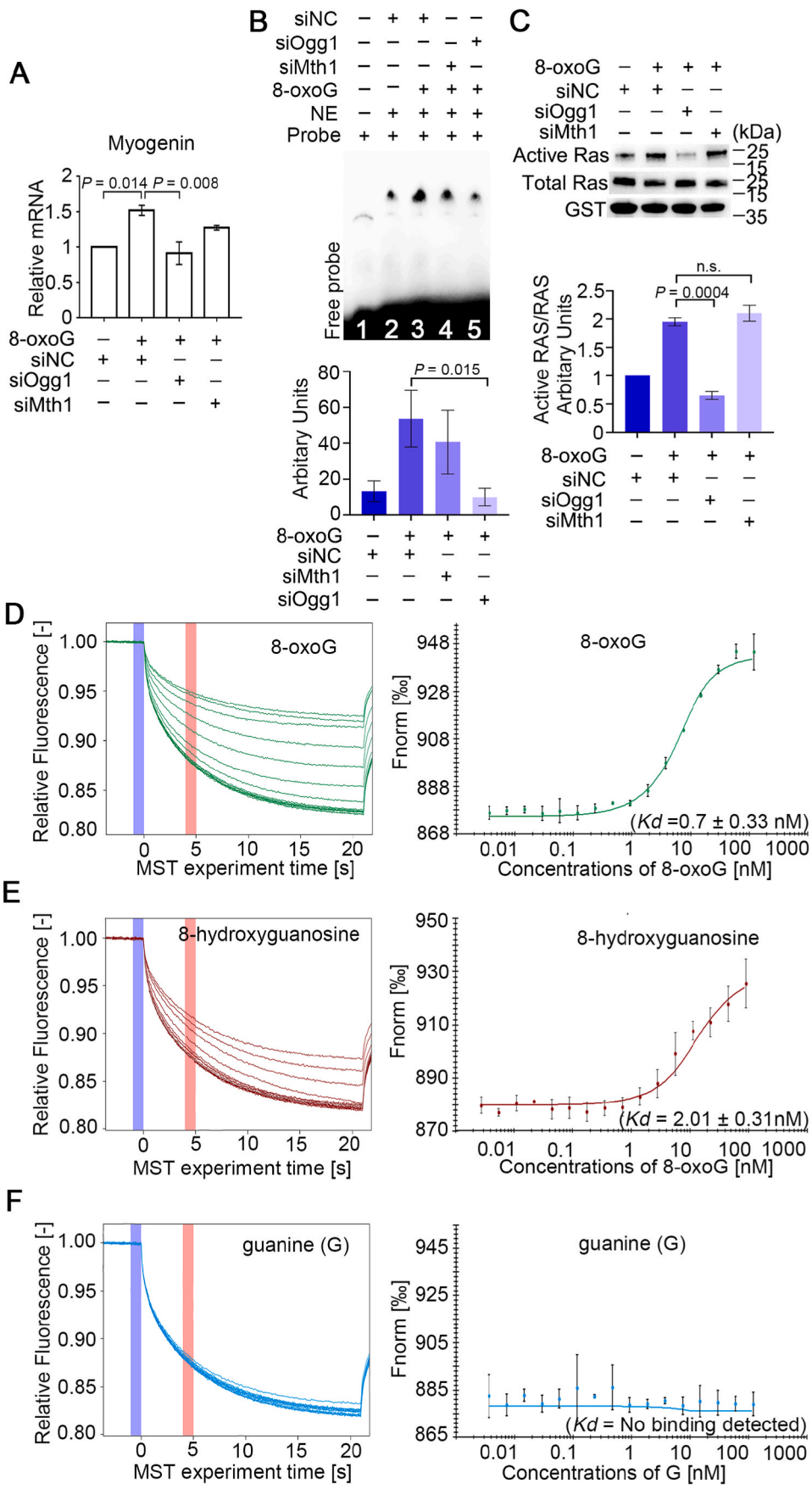

Fig. 6. OGG1 is required for 8-oxoG's role in myogenic differentiation.

A. OGG1 knock-down harnesses 8-oxoG-induced up-regulation of myogenin expression. C2C12 cells were transfected with small interfering RNA targeting *Ogg1* or *Mth1*, and mRNA levels of *Myogenin* were detected by RT-qPCR assay. One-way ANOVA and Tukey's post hoc testing was used to calculate the statistical significance.

B. OGG1 knock-down abrogates MyoD binding to MCK promoter. C2C12 cells were subjected to siRNA targeting *Ogg1* or *Mth1*, and then treated with 8-oxoG or not for 30 min. Nuclear lysates were prepared and EMSA was performed by using the MCK promoter-derived probes (100 fmol)

C. OGG1 knock-down blocks 8-oxoG-induced Ras activation. C2C12 cells were transfected with si-Ogg1 or si-Mth1 as indicated, and then treated with 8-oxoG or not. Ras activation was detected by pull-down assay. Shown are the representative images from three independent experiments, and quantitative analysis of protein-DNA binding (**B**) and Ras activation (**C**) were shown at the lower panels.

D-F. Binding of His-OGG1 with different substrates was measured by MST assays. The concentration of substrates was varied from 120 nM to 4 pM, while the concentration of the protein OGG1 was kept constant at 50 nM. Left panel shows MST traces, and right panel shows dose-response curve. The *Kd* values obtained for binding of 8-oxoG/8-hydroxyguanosine/guanine (G) to the His-OGG1 were calculated from three independent thermophoresis measurements and indicated in the individual plots as shown.

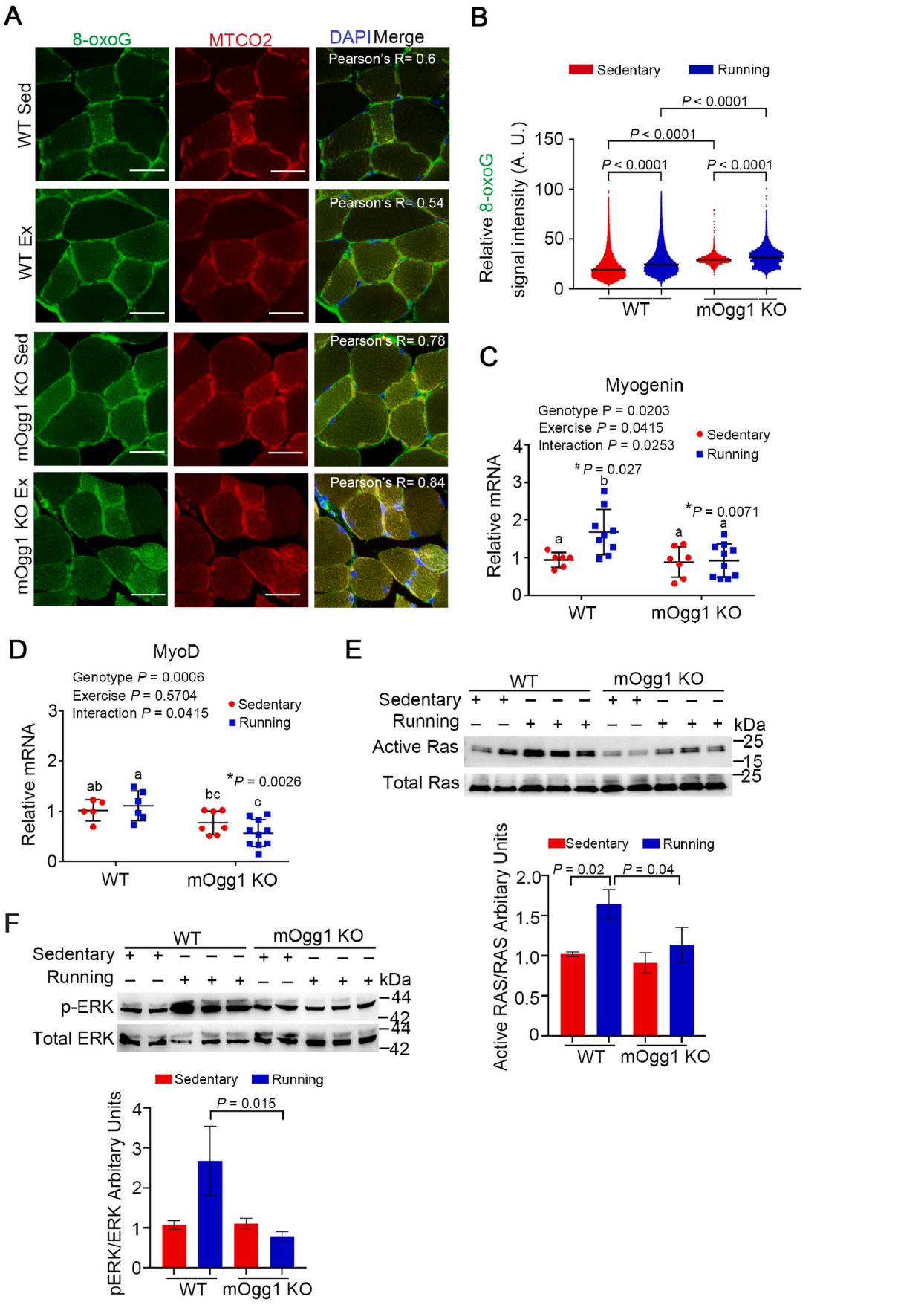

(caption on next page)

Fig. 7. 8-OxoG generation and release, Ras and MEK activation, as well as myogenic gene expression *in vivo*.
A-B. More 8-OxoG accumulation was induced in myofiber mitochondria in *Ogg1* KO mice in response to exercise. After exercise as described in method, the tibialis anterior (TA) muscle of sedentary, exercised or exercise-followed-by-rest mice was removed, cryomold, sectioned (10 μm), and processed for staining of 8-oxoG in DNA duplex (**A**). Scale bars, 100 μm. Shown are the representative images from 3 mice of each group. Statistical analysis of 8-oxoG staining was conducted as described in Methods and shown in (**B**). Data were represented as mean ± SD. One-way ANOVA and Sidak's post hoc testing was used to calculate the statistical significance. **C–F. Exercise-induced expression of *Myogenin* and activation of Ras-MEK signal pathway are compromised in TA muscle of *Ogg1* KO mice.** Wild-type (WT) and *Ogg1* KO mice were subjected to exercise as described in methods. After the last bout of running (40 min), the TA muscles were collected, and the expression of *MyoD* and *Myogenin* was measured by RT-qPCR. Two-way ANOVA and Sidak's post hoc testing was used to calculate the statistical significance. *P* values for the effects of genotype, exercise, and interaction between genotype and exercise are shown as insets. Levels not connected with the same letter are significantly different. $^{*}p$, compared with WT mice subjected to exercise; $^{\#}p$ compared with sedentary WT mice (**C**, **D**). TA muscle homogenates were prepared, active Ras was detected by pull down assay (**E**), and MEK activation was examined by western-blotting measuring ERK phosphorylation (**F**). Shown are the representative images from three independent experiments, and quantitative analysis of activation of Ras and MEK were shown at lower panels.

improve muscle function for specific or clinical setting.

5. Materials and methods

5.1. Mice

Mice were bred and cohoused, four to six mice per cage, in a specific pathogen-free facility with a standard 12 h alternate light/dark cycle at an ambient temperature of 22 ± 2°C and 30–70% humidity at the Animal Research Center of Northeast Normal University (Changchun, China). Health status of mice was determined via daily observation by technicians supported by veterinary care. All mouse experiments were conducted in accordance with the protocols for animal use, treatment, and euthanasia approved by the local ethics committee (reference number: AP2019085, the institutional animal care and use committee (IACUC) of the Northeast Normal University). *Ogg1* KO mice were kindly provided by Dr. Yusaku Nakabeppu (Division of Neurofunctional Genomics, Department of Immunobiology and Neuroscience, Medical Institute of Bioregulation, Kyushu University, Fukuoka, Japan) [47].

5.2. Acute exercise training

Armstrong training programs [19] was modified and utilized in the present study: briefly, mice were 5–10 min of running on the platform at a speed of 13 m/min with a slope of zero; thereafter, the slope angle of treadmill was set to 5°, and all mice were trained using the following exercise program: 3 min running and 2 min rest with total 40 min. Animals were acclimated with the treadmill apparatus (KW-PT, Nanjing Calvin Biotechnology, China) 1 week prior to the formal experiments. Experimental animals include 6–8weeks male C57BL/6 (WT) mice and *Ogg1* KO mice (weight 20–25 g). Generally, 24 mice were randomly divided into 4 groups: 1) without exercise (basal), 2) exercise for 40 min, 3) exercise for 40 min and rest for 40 min, and 4) exercise for 40 min and rest for 100 min. To determine the role of OGG1 in myogenic gene activation in response to exercise, after the last bout of training (40 min), the TA muscles of WT and *Ogg1* KO mice were collected, and the expression of *MyoD* and *Myogenin* was measured by RT-qPCR. Ras activation was detected by pull-down assay and MEK activation was examined by western-blotting.

5.3. Plasmids

To generate the *Myogenin*-promoter luciferase reporter plasmid, the mouse *Myogenin* promoter (−1348 ~ −65 nt, containing multiple MyoD transcription factor motifs predicted by JASPAR CORE 2018 vertebrates) was cloned from the C2C12 genome and inserted into reporter vector pGL4.2 (Promega, Madison, WI) using restriction enzyme sites *Kpn*I and *Bgl*II. Eukaryotic expressional plasmid pCS2(+)-Flag-MyoD were kindly provided by Dr. Stephen Tapscott (FHCRC, Seattle, WA). GST-MyoD, GFP-MyoD expressional plasmids were constructed by subcloning MyoD sequence into the corresponding vectors pGEX-4T-2 and pEGFP-N1. (Y156F/V) mutants were created by changing the amino acid at position 156 from tyrosine to phenylalanine/valine (Y156F/V) using a Fast Mutagenesis System kit according to the manufacturer's instructions (TRANS, FM111-01).

5.4. Cell culture and treatment

C3H10T1/2 fibroblasts and C2C12 myoblasts were cultured in growth medium (Dulbecco's modified Eagle's medium with L-glutamine (400 mM), in 10% fetal bovine serum and 1% penicillin/streptomycin at 37°C in a 5% CO_2 atmosphere. To initiate myogenic differentiation of C2C12 myoblasts, 10% fetal bovine serum was replaced with 2% horse serum (Gibco). When the cells were treated with 8-oxo-guanine (8-oxoG) or guanine (G), the reagents were dissolved as recommended by the manufacturer (Cayman Chemical, Ann Arbor, MI). Briefly, a 10 mM stock solution was prepared in 100 mM NaOH (pH 12), and the working concentration is 10 μM. Stock solutions were used immediately or stored at room temperature in dark for a maximum of 1 week [48].

5.5. 8-OxoG analyses by mass spectrometry

TA interstitial fluid was extracted from muscles immediately upon treatment using a rapid isolation procedure described previously [49,50]. Tissues were subjected to centrifugation (10 min, 800 *g*, 4°C) following placement in a 20 μm nylon mesh filter (EMD Millipore). Mass spectrometry analyses of metabolites was conducted by Shanghai ProfLeader Biotech Co, Ltd. To the sample of interstitial fluid, 3 fold volume of acetonitrile/methanol (2:1, v/v) and 50 μL of 10 ng/mL 8-hydroxyguanine-13C3 were added. The mixture was vortexed 30 s, incubated at 37 °C for 15 min, and centrifuged (15,000 *g*, 4°C) for 15 min. The supernatant was loaded on an aminopropyl cartridge which activated by methanol for further purification by solid phase extraction (SPE). The cartridge was subsequently washed by 70% aqueous methanol and the target components were eluted by 5% aqueous methanol.

The level of 8-hydroxyguanine in prepared sample was analyzed by UHPLC-MS/MS of an Agilent 1290 Infinity II UHPLC system coupled to a 6470 A Triple Quadrupole mass spectrometry (Santa Clara, CA, United States). The mobile phase consisted of (A) water with 0.1% formic acid and (B) acetonitrile. Samples was separated by Acquity BEH Amide column (100 mm × 2.1 mm, 1.7 μm, Waters), at a flow rate of 0.20 mL/min, with a gradient elution program as follows: 90% B during 0–1 min, 77% B at 8 min, 50% B at 9 min and held to 11 min, 90% B at 11.1 min and held to 14 min.

The eluted analysts were ionized in an electro spray ionization source in positive mode (ESI+). The temperatures of both source drying gas and sheath gas were 300°C and 350°C, respectively. The flow rate of source drying gas and sheath gas were 5 and 11 L/min, respectively. The pressure of nebulizer was 45 psi, and capillary voltage was 4000 V. The multiple reaction monitoring (MRM) was used to acquire data in optimized MRM transition (quantifier 168 -> 112 and qualifier 168 -> 140 for 8-hydroxyguanine, and quantifier 171 -> 114 and qualifier 168 -> 142 for 8-hydroxyguanine-13C3), fragmentor (95 V), and collision energy (21 eV for quantifier and 17 eV for qualifier). The Agilent MassHunter software (version B.08.00) was used to control instruments and acquire data.

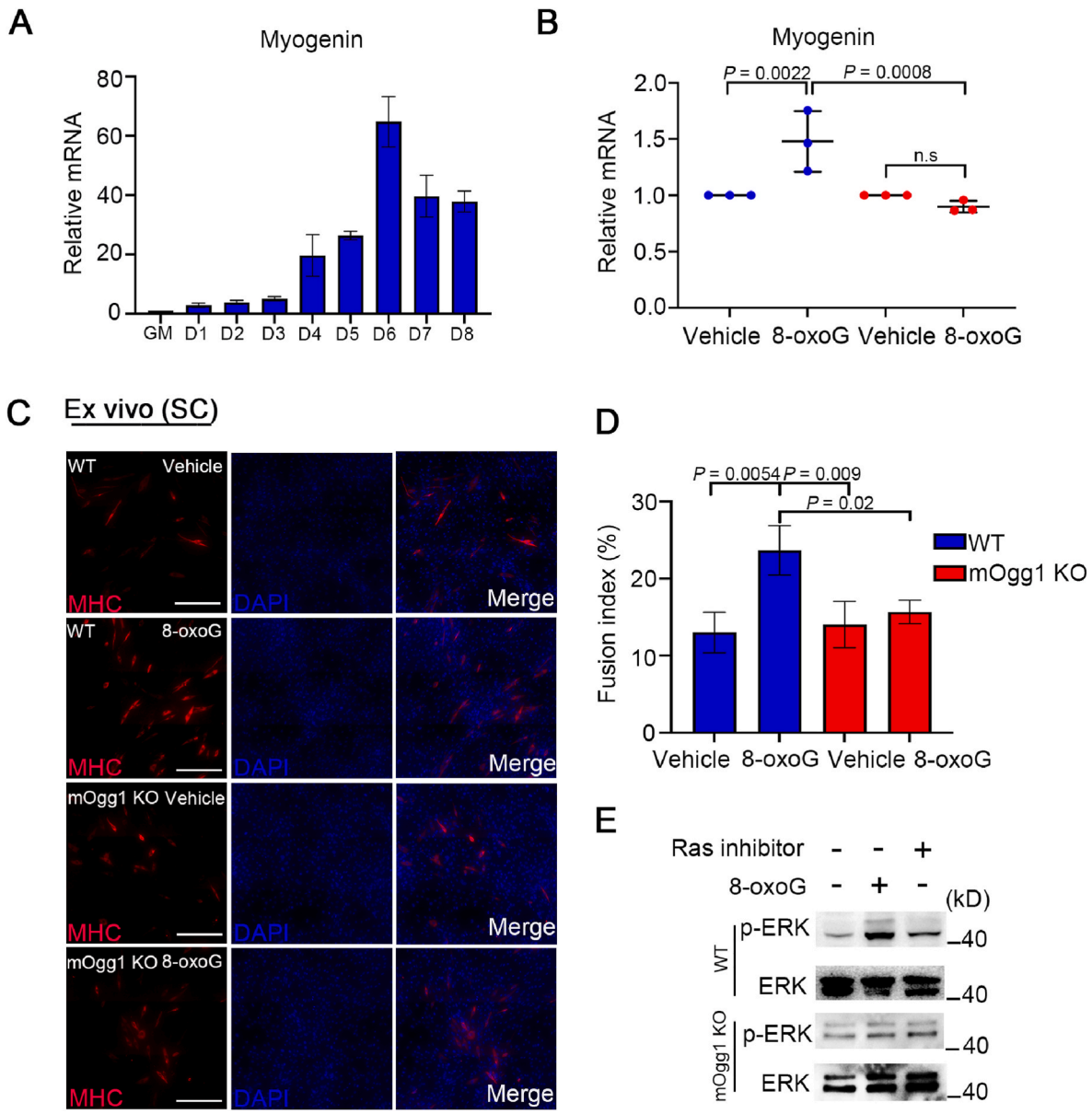

Fig. 8. 8-OxoG enhances primary myoblasts differentiation *ex vivo*.

A. The expressional dynamics of myogenin of the primary myoblasts in differentiation medium. The satellite cells were isolated as described in the Method, cultured in GM for 6 days and then shifted into DM. Thereafter, RNAs were extracted, RT-qPCR was conducted to measure the expression of *Myogenin* at different time points.

B-D. *Ogg1* depletion compromises 8-oxoG-induced expression of myogenic differentiation markers in primary myoblasts *ex vivo*. Isolation of the satellite cells from WT or *Ogg1* KO mice were performed as described in Method. Cells in DM at day 6 were exposed to 8-oxoG for 30 min, RT-qPCR was conducted to measure the expression of *MyoD* and *Myogenin.* One-way ANOVA and Tukey's post hoc testing was used to calculate the statistical significance (**B**). SCs from WT or *Ogg1* KO mice were cultured for 6 days in GM, and shifted into DM. At day 3, 8-oxoG was administrated for 4 days (once a day). The degree of differentiation was assessed by IF staining of MHC. Scale bar, 100 μm (**C**). The fusion index was calculated from cells that were immunostained for MHC. The fusion index is indicated as the value of the number of the nuclei present in myotubes divided by the number of total nuclei in MHC^{+} cells. Data were selected from 3 randomly selected microscopic fields (**D**).

E. *Ogg1* depletion decrease 8-oxoG-induced ERK activation. SCs from WT or *Ogg1* KO mice were cultured for 6 days in GM, and shifted into DM. At day 6 cells were exposed to 8-oxoG for 15 min with or without Ras inhibitors. Western-blotting was conducted to assess the level of ERK phosphorylation. Shown are the representative images from three independent experiments, and quantitative analysis of activation of MEK were shown at right panel.

5.6. RNA-seq and data analysis

For the detailed protocol, refer to the Supplementary Methods.

5.7. Quantitative real-time PCR (qRT-PCR)

To detect the mRNA levels of Total RNA was extracted using Trizol (Takara, Japan), and reverse-transcribed by using Prime Script 1st strand cDNA synthesis kit (Takara). Real-time PCR was performed by using the Prime Script RT Master Mix (Takara) and TB Green Premix Ex *Taq*II (Takara). The gene expression was calculated by $2^{-\Delta\Delta Ct}$ method. The primer sequences were shown in Supplementary Table S1.

5.8. Transfection with siRNA

The transfection of siRNA into C2C12 cells was performed in six-well

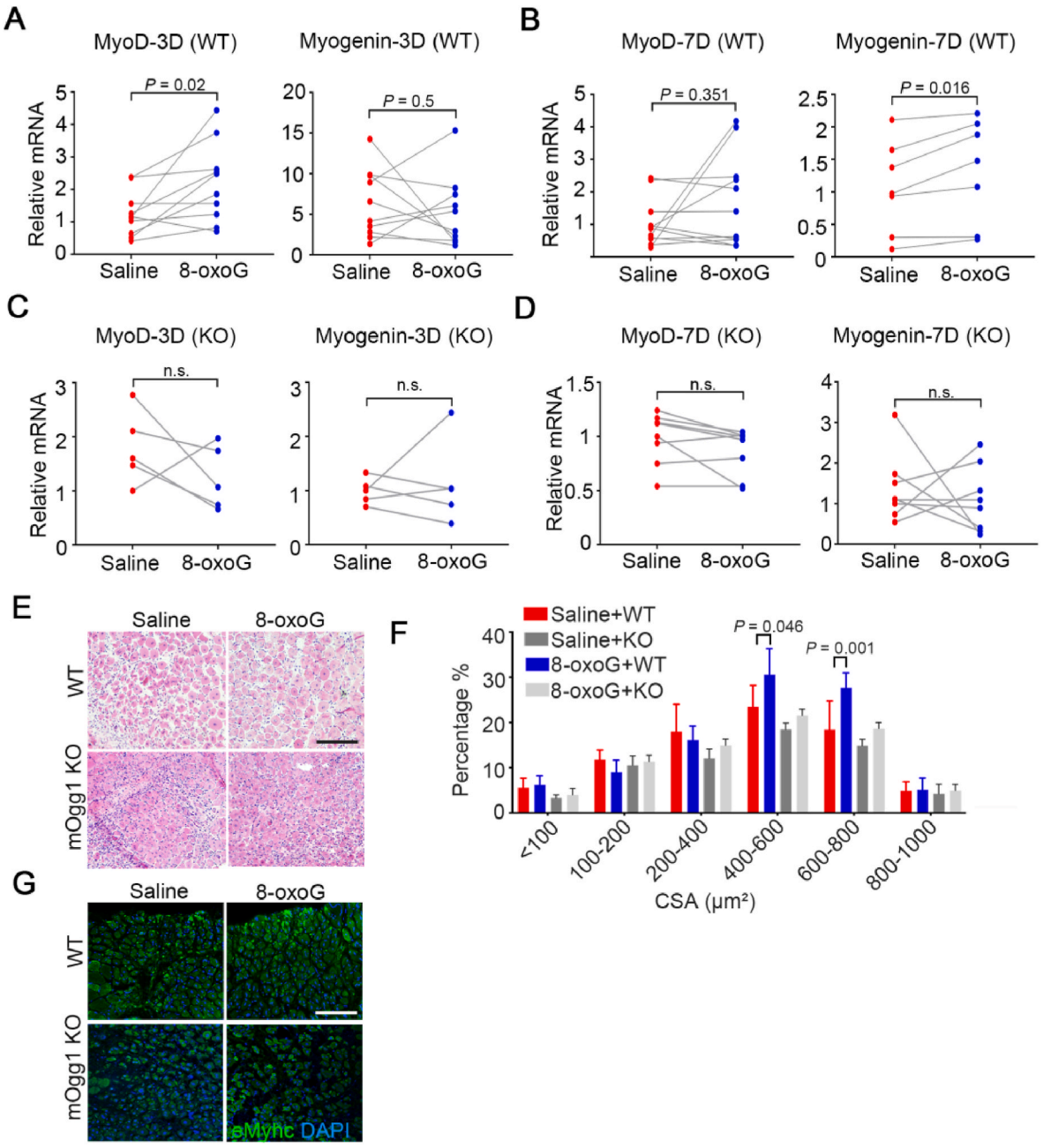

Fig. 9. Exogenously administrated 8-oxoG base promotes regeneration of injured skeletal muscle.

A-B. 8-OxoG administration promotes the expression of *MyoD* and *Myogenin* in damaged TA muscle from WT mice. After CTX injection, 8-oxoG, or saline as control, was respectively administrated to the left and right TA muscles. Samples were harvested at day 3 and 7. The mRNA levels of *MyoD* and *Myogenin* were analyzed by RT-qPCR. Each data point represents the results from an individual animal. Data were represented as mean ± SD (n = 7), and student's *t*-test (two-tailed, paired) was used to calculate the statistical significance of the difference of gene expression in left and right TA muscles from each mouse.

C-D. 8-OxoG administration failed to promote the expression of *MyoD* and *Myogenin* in damaged TA muscle from *Ogg1* KO mice. *Ogg1* KO mice were treated as described in legend for **A** and **B**. The mRNA levels of *MyoD* and *Myogenin* were analyzed by RT-qPCR as described in legend for **A** and **B**.

E-G. 8-OxoG administration accelerates the regeneration of the injured skeletal muscle. After CTX injection, 8-oxoG, or saline as control, was respectively administrated to the left and right TA muscles. Samples were harvested at day 7. H&E staining of TA muscle was performed.

The morphology of regenerated myofibers was recorded. Scale bar, 100 μm. Shown are the representative images from each group (**E**). Immunofluorescence staining of embryonic myosin heavy chain (eMyHC, green) were performed with saline or 8-oxoG treated TA muscle from WT and KO mice (**G**). Distribution of average cross-sectional area (CSA, μm^2) of the regenerated fibers was calculated as described in Methods. Data were represented as mean ± SD (n = 3), and student's *t*-test (two-tailed, unpaired) was used to calculate the statistical significance of the difference of the regenerated fibers' CSA in left and right TA muscles from each mice (**F**).

plates. The first round of transfection with siOgg1, siMth1, siMyoD or control was performed 12 h prior the culture medium was changed to differentiation medium. Cells were transfected again 48 h after the first round of transfection and the experiments were performed 2 days later. For all transfections, Lipofectamine 3000 (Invitrogen) was used following the manufacturer's protocol. SiRNA duplexes (100 pmol) was used for each well of a six-well plate, and the siRNA sequences are shown in Supplementary Table S2.

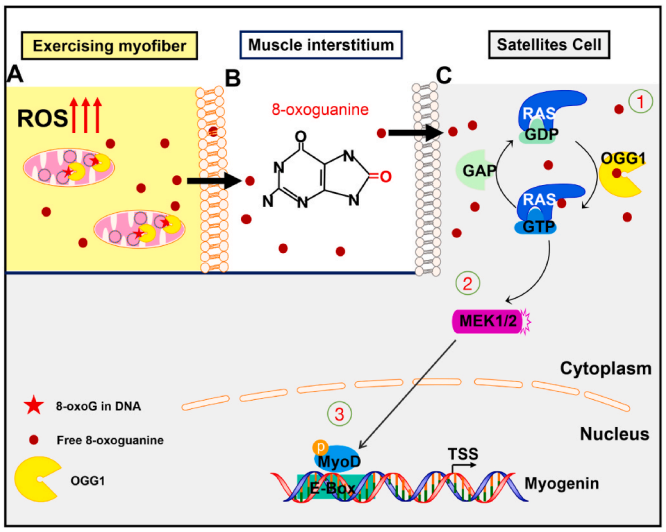

Fig. 10. Schematic illustration of the functional mechanism of 8-oxoG with OGG1 regulates muscle remodeling during exercise. Exercise-produced ROS results in generation of guanine oxidative damage lesion 8-oxoG in myofiber mitochondria **(A)**, and then 8-oxoG is excised and released into muscle interstitium, the niche for satellites cell's activation and differentiation **(B)**, After permeating into satellites cells, 8-oxoG forms complex with OGG1, inducing activation of Ras-MEK-MyoD pathway, and promoting myogenic differentiation of myoblasts **(C)**, In myoblasts, 8-oxoG is engaged by OGG1, and the complex functions as a GEF, activating Ras ①, and then MEK signal pathway ②, leading to tyrosine phosphorylation of MyoD ③, consequently up-regulating myogenic gene expression.

5.9. Immunofluorescence staining

C2C12 cells were cultured on coverslips in 24 wells plates and exposed to vehicle/G/8-oxoG for 4 days (one does per day). The coverslips were washed once with PBS (in PBS for 5 min), and then incubated in 0.25% Triton X-100 in PBS for 10 min at room temperature, and after another two washes, blocked in 3% FBS for 2 h. The coverslips were then incubated with anti-MHC antibody (1:200) at 4°C overnight, followed by TRITC-conjugated goat anti-mouse fluorescent secondary antibody (1:200) for 1 h. After three times of washing with PBS, cells were incubated with DAPI (D1306, Invitrogen) (1:8000) for 5 min to visualize cell nuclei.

For staining of tissue sections, O.C.T compound was used to quickly embed fresh TA muscles. Freeze the tissues immediately to set cryomold on metal block in liquid nitrogen. Keep the specimens at −80°C until use. Serial sections (10 μm thick) were cut on cryostat. Each section was collected as a free-floating section in slide, and processed immediately for immunodetection. The sections were then permeated with 0.5% Triton X-100 in PBS for 10 min [51], and then washed twice with PBST. After blocking with 2% FBS in PBST at RT for 10 min. Sections were then incubated with mouse anti-8-oxoG (EMD Millipore Corp, MAB3560) and anti-rabbit-mitochondria marker MTCO2 (Proteintech, 55070-1-AP). Antibody against mouse-eMyhc was used to label actively regenerating fiber. Confocal images were obtained using an inverted LSM750 META confocal microscope (Carl Zeiss) using a 63 × oil object. An 8-oxoG index was calculated as immunofluoresce intensity of 8-oxoG per MTCO2-positive area of tissue, using software in NIS Elements (Nikon, Version 5.01).

5.10. Myotube fusion index

The efficiency of C2C12 differentiation was determined by the fusion index as described previously [52]. Briefly, 30 fields of each sample were chosen, and MHC^+ cells were counted. The fusion index is indicated as the value of the number of the nuclei present in myotubes divided by the number of total nuclei in MHC^+ cells.

5.11. Luciferase reporter assays

C3H10T1/2 cells were seeded in the 24-well plates overnight in the absence of antibiotics. The cells were then transfected *Myogenin* promoter-driven firefly luciferase reporter plasmid or control vector (pGL4.2) and Renilla luciferase reporter plasmid (an internal control, Promega), as well as the expressional plasmid Flag-MyoD, using Lipofectamine 2000 transfection reagent (Invitrogen). Cells were challenged with or without 8-oxoG/G and 6 h later, lysed in 100 μL passive lysis buffer, and then the extracts (20 μL) were used for luciferase activity using a Dual Luciferase Reporter Assay kit (Promega). To signify the rapid transcriptional activation of *Myogenin*, RNA was extracted after the cell were challenged with or without 8-oxoG/G for 30 min. Firefly luciferase mRNA levels were measured by RT-qPCR and calibrated to that of Renilla. Primers used were shown in Supplementary Table S1.

5.12. Subcellular fractionation and western blot

C2C12 cells were lysed in lysis buffer [53] for 30 min on ice. Lysates were centrifuged at 12,000 *g* for 20 min at 4°C, and the supernatants were taken as the whole-cell extract (WE). Cytoplasmic and nuclear fractions were prepared using the CelLytic NuCLEAR Extraction kit (Sigma, NXTRACT) following the manufacturer's guidance. Briefly, cells were lysed with cytosolic lysis buffer for 20 min, and then centrifuged (11,000 *g*, 1 min, 4°C), and supernatants were collected (CE). The pellets were washed twice with cytosolic lysis buffer and lysed with extraction buffer. Nuclear lysates were clarified by centrifugation (21,000 *g*, 5 min, 4°C), and the supernatants were collected (NE). Then, 20 μg of protein from each sample was mixed with 2 × SDS sample buffer, resolved by SDS–polyacrylamide gel, and then transferred on nitrocellulose (NC) membranes. Each NC membrane blot was sealed with 5% skimmed milk powder for 1 h at RT and incubated with primary antibodies overnight at 4°C. After three washes in TBST (Tris-buffered saline containing Tween 20), the membranes were incubated with HRP-conjugated secondary antibody for 1 h and detected by freshly made ECL (enhanced chemiluminescence) solution. The primary antibodies were as follow: anti-MHC (1:200), anti-Ras (1:1000), anti-RhoA (1:1000), anti-Cdc42 (1:1000), anti-Rac1 (1:1000), anti-ERK (1:3000), anti-p38 (1:3000), anti-pERK (1:3000), anti-pp38 (1:3000), anti-JNK (1:1000), anti-pJNK (1:1000), anti-pTyr (1:500), anti-MyoD (1:1000), anti-Ogg1 (1:1000), anti-Mth1 (1:500), anti-GST (1:3000), anti-GFP (1:3000), anti-GAPDH (1:3000).

5.13. Chromatin immunoprecipitation assay

C2C12 cells were grown to a final count of 5–10 × 10^7 cells for each sample. Cells were cross-linked in 1% formaldehyde at RT for 5 min and then added 125 nM Glysine for 5 min. After washing with PBS, the cells were resuspended and lysed in lysis buffers and sonicated to solubilize and shear the crosslinked DNA. Sonicated chromatin was diluted to a final SDS concentration of 0.1%, and for each sample, 500 μL of DNA-protein complexe (near 25 μg of genomic DNA fragment per sample) were immunoprecipitated using 2 μg of MyoD Ab at 4°C overnight, then incubated with 30 μL of magnetic beads for 3 h. The precipitates were washed three times, decrosslinked, and subjected to RT-qPCR following the manufacturer's instructions for the Simple ChIP Enzymatic Chromatin IP Kit (Cell signaling technology, US, #9003). The primer sequences were shown in Supplementary Table S3.

5.14. Expression and purification of the recombinant proteins

GST and GST-MyoD proteins were induced in BL21 (DE3) of *Escherichia coli*. The protein expression was achieved by adding 1 mM

IPTG (isopropyl-b-D-thiogalactopyranoside) and 40 μM $ZnSO_4$ at 37°C overnight. The culture was centrifuged at 12,000 rpm/min for 5 min, and the pellet was resuspended in chilled lysates buffer (20 mM HEPES, 120 mM NaCl, 10% Glycerin, 2 mM EDTA, protease inhibitor cocktail) and homogenized by sonication. The lysate was centrifuged at 14,000 rpm for 20 min at 4°C. The supernatant was then applied to glutathione-Sepharose 4 B beads (GE Healthcare). The protein-loaded 4 B beads were washed with 5 vol of PBS and 5 vol of TEN100 (20 mM Tirs-HCl (pH 7.5), 0.1 mM EDTA (pH 8.0), 100 mM NaCl) and NETN (20 mM Tirs-HCl (pH 7.5), 0.1 mM EDTA (pH 8.0), 100 mM NaCl, 0.5% NP-40). Free GST and GST-MyoD proteins were purified and eluted in 100 μL buffer (50 mM Tris-HCl (pH 8.0), 100 mM KCl and 40 mM glutathione, and protease inhibitor cocktail) and used for EMSA.

5.15. Electrophoretic mobility shift assay (EMSA)

The EMSA analysis was performed using the LightShift chemiluminescent EMSA kit (ThermoFisher Scientific, 20,148). GST-fused Recombinant MyoD (40, 30, 20, 10, 5 or 2.5 nM) or nuclear extracts (1 μg) were mixed with 100 fmol of Biotin-labeled and canonical E box-containing oligonucleotide probe in a binding buffer (20 mM HEPEs (pH 7.6), 1.5 mM $MgCl_2$, 10 mM KCl, 1 mM EDTA, 1 mM dithiothreitol, 1 mg/ml BSA) with 1 μg poly (dI-dC) in a total volume of 10 μL. After incubation at RT for 20 min, the entire reaction was loaded on a 6% non-denaturing poly acrylamide-Tris-borate-EDTA (TBE) gel and run at 100 V for 2 h at 4°C. The sequence information of the probe was shown in Supplementary Table S4.

5.16. Oligonucleotide incision assay

To examine the lesion incision abilities of OGG1, a 37-mer oligonucleotide containing an 8-oxoG at position 16 and labeled at the 3′ end with Cy5 was used (Supplementary Table S5). For the incision assay, 200 fmol Cy5-labeled probe was incubated with homogenates of TA tissue (10 μg) from sedentary and post-exercise mice in a total volume of 10 μL comprising 10 mM of Tris-HCl (pH 7.5), 10 mM of NaCl, 1 mM of EDTA, 1 mg/ml BSA, and 1 mM of DTT. After incubation for 20 min at 37°C, the reaction was halted by adding 10 μL loading buffer (containing 8 μL of formamide, 10 mM of NaOH) and heating for 5 min at 95°C. The reaction mixtures were separated in a 20% of polyacrylamide gel containing 8 M of urea in Tris-borate-EDTA buffer (pH 8.4). Fluorescence detection of the DNA bands was visualized via BIO-RAD ChemiDoc™ MP Imaging System.

5.17. Small GTPase activity assay

To measure the level of the activity of small GTPases (Ras, Rac1/Cdc42 and RhoA), C2C12 cells were treated with vehicle or 10 μM 8-oxoG for 0, 3, 6, 9, 12 min. After treatment, cells were immediately harvested on ice in lysis buffer containing 25 mM Tris-Cl (pH 7.4), 150 mM NaCl, 50 mM $MgCl_2$, 1 mM NaF, 1 mM of $NaVO_3$, 1% IGEPAL, and 1 mM protease inhibitors. Lysates were vortexed, incubated on ice for 5 min and then clarified by centrifugation at 15,000 rpm for 15 min at 4°C, and 500 μg of protein was used in a pull-down assay with GST-Raf1-RBD (for Ras), GST-Pak1-RBD (for Rac1/Cdc42), or GST-Rhotekin-RBD (for RhoA) beads for 1 h with rotation at 4°C. The protein-coated beads were washed thrice with lysis buffer and then suspended in 2 × loading buffer. The resulting pull-down was then subjected to western-blotting to measure the activity Ras, Rac1/Cdc42 and RhoA by using anti-Ras, anti-Rac1/Cdc42 and anti-RhoA antibodies.

5.18. Microscale thermophoresis (MST)

The MST experiments were performed using a Monolith NT.115 instrument (NanoTemper) as described previously [54]. For each binding experiment recombinant Human OGG1/MTH1 was diltued to 50 nM in MST buffer (PBS with 3 mM DTT, 0.05% Tween-20, and 0.2% Prionex). A series of 16 tubes with 8-oxoG/G/8-hydroxyguanosine were prepared in MST buffer, producing 8-oxoG/G/8-hydroxyguanosine ligand concentrations ranging from 120 nM to 4 pM. The reaction was mixed by pipetting, incubated for 30 min at RT followed by centrifugation at 10,000×*g* for 10 min. Capillary forces were used to load the samples into Monolith NT.115 Premium Capillaries (NanoTemper Technologies). Measurements were performed using a Monolith NT.115Pico instrument (NanoTemper Technologies) at an ambient temperature of 25°C. Instrument parameters were adjusted to 20% LED power, medium MST power and MST on-time of 10 s. An initial fluorescence scan was performed across the capillaries to determine the sample quality and afterwards 16 subsequent thermophoresis measurements were performed. The *Kd* values were calculated using MO. Affinity Analysis software, (NanoTemper Technologies). The data presented here was repeated at three times confirming the results.

5.19. Isolation and identification of muscle satellite cells

Primary myoblasts were purified from C57BL/6 mice by magnetic cell separation (MACS) [55]. Briefly, dissected muscles from the hind limbs were minced and dissociated in a collagenase/dispase solution (0.5% collagenase type II, 1% dispase in PBS) and incubated for 40 min at 37°C with regularly shaking during the incubation. Digestion was terminated by addition of 20% FBS. Samples were centrifuged at 500×*g* for 1 min. Cells were filtered, centrifuged, and resuspended in MACS buffer (0.5% BSA, 2 mM EDTA in PBS). Satellite Cell Isolation Cocktail (Miltenyi Biotec), containing microbeads conjugated to CD11b, SCA-1, CD45 and CD31 antibodies, was added for 15 min. Cell suspensions were loaded onto a LD column (Miltenyi Biotec) in the magnetic field of a VarioMACS separator (Miltenyi Biotec) and rinsed with MACS buffer. Column flow-through (containing the lineage-negative cells) was collected and stained with anti-α7-INTEGRIN MicroBeads (Miltenyi Biotec) for 15 min. Cells were loaded onto a MS column (Miltenyi Biotec) and washed 3 times with MACS buffer. Flow-through was discarded, and the column was flushed to collect satellite cells and myoblasts. Cells were cultured at 37°C in Ham's F-10 medium (40%) and DMED (40%) supplemented with 20% fetal bovine serum, 1% penicillin/streptomycin, and 2.5 ng/ml bFGF.

After six days, medium was changed to differentiation medium (2% horse serum, 98% DMEM). To identify the myoblast lineage of the culture, cells were washed with PBS, and fixed with 4% formaldehyde/PBS at room temperature for 15 min. After washing three times with PBS, cells were treated with 0.25% Triton X-100/PBS (containing 5 mM EDTA and 2% FBS) for 5 min and washing for three times, followed by incubation with anti-MyoD (1:200) at 4°C overnight. After eliminating the excessive primary antibodies with PBS, cells were incubated with TRITC-conjugated secondary antibodies (1:200) for 1 h. After washing three times in PBS, specimens were labeled with DAPI for 5 min. Finally, cells were washed twice with PBS for 5 min and fluorescence-labeled cells were observed under the fluorescence microscope. The images were visualized and captured by an Eclipse Ti2 microscope (Nikon Instruments Inc, Melville, NY).

5.20. Muscle damage and regeneration

For muscle injury, Six-to-eight week male C57BL/6 (WT) mice and *Ogg1* KO mice (weight 20–25 g) were anesthetized with inhalation of 1–2% isoflurane (Vedco), and treated with 25 μL of 10 μM (in pyrogen-free saline) cardiotoxin VII4 (CTX, Sigma-Aldrich) via intramuscular injection into the anterior compartments of both hindlimbs. Mice (n = 5 mice/time point) were sacrificed on day 1, 3, 7, 9 and 11 after CTX-induced injury. TA muscles were collected and mRNA levels of *MyoD* and *Myogenin* of samples were measured. To detect the role of 8-oxoG in muscle regeneration, after CTX-induced injury, 20 μL of vehicle (1 mM NaOH in saline) and 8-oxoG (100 μM) were injected intramuscularly

into the left and right TA of these mice, respectively, on day 1, 2, 3, 5 and 7. TA muscles were collected on day 3 and 7, mRNA levels of *MyoD* and *Myogenin* of samples were measured; or in other experiments, TA muscles were collected on day 7, and placed in 10% neutral buffered formalin (NBF) for histological examination to confirm the extent of muscle regeneration, or embedded within Tissue-Tek O.C.T for immunolfluorescence staining of eMyHC-positive regenerated myofibers.

5.21. Hematoxylin and eosin (H&E) staining

H&E staining was performed according to the method described previously [47]. Skeletal muscle samples were immersion-fixed in 4% paraformaldehyde and embedded with paraffin, sectioned (5 μm). H&E staining was processed to show the morphology of regenerated myofibers. Randomly, five fields of each sample with no bias were captured at a magnification of 10× using an Olympus AX70 microscope (Olympus Optical, Japan). The centrally nucleated fibers, representative for the regenerated ones, were counted. The average cross-sectional area (CSA, μm^2) was analyzed by using Image J software (1.4.3 V, US National Institutes of Health). Because errors in fiber border recognition might occur (i.e. either the fibers might not be recognized or several fibers/non-fibre regions might be interpreted as a single fibre), a manual correction of myofiber border misinterpretation was performed [56]. The CSA is indicated as the value of the cross area of the total counted fibers divided by the number of the fibers.

5.22. Statistical analysis

Fluorescence quantification and normalization were performed using ImageJ software. All data are representative of three independent experiments and shown as mean ± standard deviaton (SD). Differences between two groups were analyzed by two-tailed Student's *t*-test paired or unpaired. One-way analysis of variance (ANOVA) was performed for all experiments that require a comparison between three or more groups within one categorical variable followed by a Sidak's post hoc test or Tukey's post hoc test. To test the effect of two independent variables on a dependent variable, two-way ANOVA followed by Tukey's post hoc test or Sidak's post hoc test was used. In all analyses, significance was accepted with $P < 0.05$ and analyses were performed using GraphPad Prism 7.00 software (GraphPad Software Inc, CA).

Author contributions

X.Z, X.B, IB, and Z.R. conceptualized the study. M.T, X.Z. and X.B. designed the methodology. X.B, IB, Y.N. and Z.R. supervised the experiments. X.B. and X.Z. wrote the manuscript. X.Z, W.Z, Y.H, J.W, F.H, J.H, J.X, W.H. and R.W. performed the experiments. Z.Z. performed the RNA-seq data anslyses. X.Z. and W.H.Z. performed formal statistics analyses. X.B, R.W. and IB. were responsible for funding acquisition. All authors reviewed and edited the manuscript.

Declaration of competing interests

The authors declare no competing interests.

Data availability

Data will be made available on request.

Acknowledgements

We appreciate Dr. Stephen Tapscott (FHCRC, Seattle, WA) for providing plasmid pCS2 (+)-Flag-MyoD. And we thank Mr. Genda Zhao (Changchun New Oriental School) for his help with language editing. This work was supported by grants from the National Natural Science Foundation of China (grant numbers: 31970686 and 32170591 to X.B., 31900557 to R.W.), and grants from United States National Institute of Allergic and Infectious Diseases (Grant no. AI062885 to IB.).

Appendix A. Supplementary data

Supplementary data to this article can be found online at https://doi.org/10.1016/j.redox.2023.102634.

References

[1] John A. Hawley, M. Hargreaves, Michael J. Joyner, Juleen R. Zierath, Integrative biology of exercise, Cell 159 (4) (2014) 738–749.
[2] Z. Radak, K. Suzuki, A. Posa, Z. Petrovszky, E. Koltai, I. Boldogh, The systemic role of SIRT1 in exercise mediated adaptation, Redox Biol. 35 (2020) 101467, 101467.
[3] B. Egan, Juleen R. Zierath, Exercise metabolism and the molecular regulation of skeletal muscle adaptation, Cell Metabol. 17 (2) (2013) 162–184.
[4] H. Quan, E. Koltai, K. Suzuki, A.S. Aguiar, R. Pinho, I. Boldogh, I. Berkes, Z. Radak, Exercise, redox system and neurodegenerative diseases, Biochim. Biophys. Acta (BBA) - Mol. Basis Dis. 1866 (10) (2020), 165778.
[5] K. Contrepois, S. Wu, K.J. Moneghetti, D. Hornburg, S. Ahadi, M.-S. Tsai, A. A. Metwally, E. Wei, B. Lee-McMullen, J.V. Quijada, S. Chen, J.W. Christle, M. Ellenberger, B. Balliu, S. Taylor, M.G. Durrant, D.A. Knowles, H. Choudhry, M. Ashland, A. Bahmani, B. Enslen, M. Amsallem, Y. Kobayashi, M. Avina, D. Perelman, S.M. Schüssler-Fiorenza Rose, W. Zhou, E.A. Ashley, S. B. Montgomery, H. Chaib, F. Haddad, M.P. Snyder, Molecular choreography of acute exercise, Cell 181 (5) (2020) 1112–1130.e16.
[6] M. Dizdaroglu, Oxidative damage to DNA in mammalian chromatin, Mutation Research/DNAging 275 (3) (1992) 331–342.
[7] M. Sankar, K.H. Tapas, R. Rabindra, I. Shogo, B. Tapan, L. Julie, B. Istvan, I. Tadahide, Complexities of DNA base excision repair in mammalian cells, Mol. Cell. 7 (3) (1997) 305–312.
[8] C.-W. Hu, M.-R. Chao, C.-H. Sie, Urinary analysis of 8-oxo-7,8-dihydroguanine and 8-oxo-7,8-dihydro-2'-deoxyguanosine by isotope-dilution LC-MS/MS with automated solid-phase extraction: study of 8-oxo-7,8-dihydroguanine stability, Free Radic. Biol. Med. 48 (1) (2010) 89–97.
[9] H.E. Poulsen, L.L. Nadal, K. Broedbaek, P.E. Nielsen, A. Weimann, Detection and interpretation of 8-oxodG and 8-oxoGua in urine, plasma and cerebrospinal fluid, Biochim. Biophys. Acta Gen. Subj. 1840 (2) (2014) 801–808.
[10] P. Seale, L.A. Sabourin, A. Girgis-Gabardo, A. Mansouri, P. Gruss, M.A. Rudnicki, Pax7 is required for the specification of myogenic satellite cells, Cell 102 (6) (2000) 777–786.
[11] S.N. Shapira, H.R. Christofk, Metabolic regulation of tissue stem cells, Trends Cell Biol. 30 (7) (2020) 566–576.
[12] P. Feige, C.E. Brun, M. Ritso, M.A. Rudnicki, Orienting muscle stem cells for regeneration in homeostasis, aging, and disease, Cell Stem Cell 23 (5) (2018) 653–664.
[13] K. Papanikolaou, A.S. Veskoukis, D. Draganidis, I. Baloyiannis, C.K. Deli, A. Poulios, A.Z. Jamurtas, I.G. Fatouros, Redox-dependent regulation of satellite cells following aseptic muscle trauma: implications for sports performance and nutrition, Free Radic. Biol. Med. 161 (2020) 125–138.
[14] Z. Radák, M. Atalay, J. Jakus, I. Boldogh, K. Davies, S. Goto, Exercise improves import of 8-oxoguanine DNA glycosylase into the mitochondrial matrix of skeletal muscle and enhances the relative activity, Free Radic. Biol. Med. 46 (2) (2009) 238–243.
[15] Z. Radak, Z. Bori, E. Koltai, I.G. Fatouros, A.Z. Jamurtas, I.I. Douroudos, G. Terzis, M.G. Nikolaidis, A. Chatzinikolaou, A. Sovatzidis, S. Kumagai, H. Naito, I. Boldogh, Age-dependent changes in 8-oxoguanine-DNA glycosylase activity are modulated by adaptive responses to physical exercise in human skeletal muscle, Free Radic. Biol. Med. 51 (2) (2011) 417–423.
[16] I. Boldogh, G. Hajas, L. Aguilera-Aguirre, M.L. Hegde, Z. Radak, A. Bacsi, S. Sur, T. K. Hazra, S. Mitra, Activation of ras signaling pathway by 8-oxoguanine DNA glycosylase bound to its excision product, 8-oxoguanine, J. Biol. Chem. 287 (25) (2012) 20769–20773.
[17] J. Luo, K. Hosoki, A. Bacsi, Z. Radak, M.L. Hegde, S. Sur, T.K. Hazra, A.R. Brasier, X. Ba, I. Boldogh, 8-Oxoguanine DNA glycosylase-1-mediated DNA repair is associated with Rho GTPase activation and α-smooth muscle actin polymerization, Free Radic. Biol. Med. 73 (2014) 430–438.
[18] L. Sylow, M. Kleinert, E.A. Richter, T.E. Jensen, Exercise-stimulated glucose uptake-regulation and implications for glycaemic control, Nat. Rev. Endocrinol. 13 (3) (2017) 133–148.
[19] J.D. Conner, T. Wolden-Hanson, L.S. Quinn, Assessment of murine exercise endurance without the use of a shock grid: an alternative to forced exercise, JoVE 90 (2014) e51846, e51846.
[20] C. Henríquez-Olguin, J.R. Knudsen, S.H. Raun, Z. Li, E. Dalbram, J.T. Treebak, L. Sylow, R. Holmdahl, E.A. Richter, E. Jaimovich, T.E. Jensen, Cytosolic ROS production by NADPH oxidase 2 regulates muscle glucose uptake during exercise, Nat. Commun. 10 (1) (2019) 4623, 4623.
[21] G. Hajas, A. Bacsi, L. Aguilera-Aguirre, M.L. Hegde, K.H. Tapas, S. Sur, Z. Radak, X. Ba, I. Boldogh, 8-Oxoguanine DNA glycosylase-1 links DNA repair to cellular signaling via the activation of the small GTPase Rac1, Free Radic. Biol. Med. 61 (2013) 384–394.

[22] P.S. Zammit, Function of the myogenic regulatory factors Myf5, MyoD, Myogenin and MRF4 in skeletal muscle, satellite cells and regenerative myogenesis, Semin. Cell Dev. Biol. 72 (2017) 19–32.
[23] C.A. Berkes, D.A. Bergstrom, B.H. Penn, K.J. Seaver, P.S. Knoepfler, S.J. Tapscott, Pbx marks genes for activation by MyoD indicating a role for a homeodomain protein in establishing myogenic potential, Mol. Cell. 14 (4) (2004) 465–477.
[24] C. Jo, S.-J. Cho, S.A. Jo, Mitogen-activated protein kinase kinase 1 (MEK1) stabilizes MyoD through direct phosphorylation at tyrosine 156 during myogenic differentiation, J. Biol. Chem. 286 (21) (2011) 18903–18913.
[25] F. Lluís, E. Perdiguero, A.R. Nebreda, P. Muñoz-Cánoves, Regulation of skeletal muscle gene expression by p38 MAP kinases, Trends Cell Biol. 16 (1) (2006) 36–44.
[26] P. Feige, M.A. Rudnicki, Isolation of satellite cells and transplantation into mice for lineage tracing in muscle, Nat. Protoc. 15 (3) (2020) 1082–1097.
[27] O. Guardiola, G. Andolfi, M. Tirone, F. Iavarone, S. Brunelli, G. Minchiotti, Induction of acute skeletal muscle regeneration by cardiotoxin injection, JoVE 119 (2017), 54515.
[28] B.K. Pedersen, M.A. Febbraio, Muscles, exercise and obesity: skeletal muscle as a secretory organ, Nat. Rev. Endocrinol. 8 (8) (2012) 457–465.
[29] S. Joanisse, T. Snijders, J.P. Nederveen, G. Parise, The impact of aerobic exercise on the muscle stem cell response, Exerc. Sport Sci. Rev. 46 (2018) 180–187.
[30] A. Chiche, I. Le Roux, M. von Joest, H. Sakai, S.B. Aguín, C. Cazin, R. Salam, L. Fiette, O. Alegria, P. Flamant, S. Tajbakhsh, H. Li, Injury-induced senescence enables in vivo reprogramming in skeletal muscle, Cell Stem Cell 20 (3) (2017) 407–414.e4.
[31] Y. Tsuchiya, Y. Kitajima, H. Masumoto, Y. Ono, Damaged myofiber-derived metabolic enzymes act as activators of muscle satellite cells, Stem Cell Rep. 15 (4) (2020) 926–940.
[32] Y.-M. Shih, M.S. Cooke, C.-H. Pan, M.-R. Chao, C.-W. Hu, Clinical relevance of guanine-derived urinary biomarkers of oxidative stress, determined by LC-MS/MS, Redox Biol. 20 (2019) 556–565.
[33] C.R. Crawford, C. Patel Dh Fau - Naeve, J.A. Naeve C, Fau - belt, J.A. Belt, Cloning of the human equilibrative, nitrobenzylmercaptopurine riboside (NBMPR)-insensitive nucleoside transporter ei by functional expression in a transport-deficient cell line, J. Biol. Chem. 273 (1998) 5288–5293.
[34] S.M. Naes, S. Ab-Rahim, M. Mazlan, A. Abdul Rahman, Equilibrative nucleoside transporter 2: properties and physiological roles, BioMed Res. Int. 2020 (2020), 5197626.
[35] E. Gredinger, A.N. Gerber, Y. Tamir, S.J. Tapscott, E. Bengal, Mitogen-activated protein kinase pathway is involved in the differentiation of muscle cells, J. Biol. Chem. 273 (17) (1998) 10436–10444.
[36] C. Jo, B.G. Jang, S.A. Jo, MEK1 plays contrary stage-specific roles in skeletal myogenic differentiation, Cell. Signal. 21 (12) (2009) 1910–1917.
[37] F. Lluís, E. Ballestar, M. Suelves, M. Esteller, P. Muñoz-Cánoves, E47 phosphorylation by p38 MAPK promotes MyoD/E47 association and muscle-specific gene transcription, EMBO J. 24 (5) (2005) 974–984.
[38] S.J. Lessard, T.L. MacDonald, P. Pathak, M.S. Han, V.G. Coffey, J. Edge, D.A. Rivas, M.F. Hirshman, R.J. Davis, L.J. Goodyear, JNK regulates muscle remodeling via myostatin/SMAD inhibition, Nat. Commun. 9 (1) (2018) 3030, 3030.
[39] S.-J. Xie, J.-H. Li, H.-F. Chen, Y.-Y. Tan, S.-R. Liu, Y. Zhang, H. Xu, J.-H. Yang, S. Liu, L.-L. Zheng, M.-B. Huang, Y.-H. Guo, Q. Zhang, H. Zhou, L.-H. Qu, Inhibition of the JNK/MAPK signaling pathway by myogenesis-associated miRNAs is required for skeletal muscle development, Cell Death Differ. 25 (9) (2018) 1581–1597.
[40] E.N. Olson, G. Spizz, M.A. Tainsky, The oncogenic forms of N-ras or H-ras prevent skeletal myoblast differentiation, Mol. Cell Biol. 7 (6) (1987) 2104–2111.
[41] J. Suzuki, Y. Kaziro, H. Koide, Positive regulation of skeletal myogenesis by R-Ras, Oncogene 19 (9) (2000) 1138–1146.
[42] J. Suzuki, Y. Kaziro, H. Koide, An activated mutant of R-Ras inhibits cell death caused by cytokine deprivation in BaF3 cells in the presence of IGF-I, Oncogene 15 (14) (1997) 1689–1697.
[43] M. Schaks, G. Giannone, K. Rottner, Actin dynamics in cell migration, Essays Biochem. 63 (5) (2019) 483–495.
[44] P.-C. Pao, D. Patnaik, L.A. Watson, F. Gao, L. Pan, J. Wang, C. Adaikkan, J. Penney, H.P. Cam, W.-C. Huang, L. Pantano, A. Lee, A. Nott, T.X. Phan, E. Gjoneska, S. Elmsaouri, S.J. Haggarty, L.-H. Tsai, HDAC1 modulates OGG1-initiated oxidative DNA damage repair in the aging brain and Alzheimer's disease, Nat. Commun. 11 (1) (2020) 2484, 2484.
[45] L. Forcina, M. Cosentino, A. Musarò, Mechanisms regulating muscle regeneration: insights into the interrelated and time-dependent phases of tissue healing, Cells 9 (5) (2020) 1297.
[46] N.V. Senyavina, T.N. Gerasimenko, K.A. Fomicheva, S.A. Tonevitskaya, A. D. Kaprin, Localization and expression of nucleoside transporters ENT1 and ENT2 in polar cells of intestinal epithelium, Bull. Exp. Biol. Med. 160 (6) (2016) 771–774.
[47] K. Sakumi, M.Tominaga Y. Fau - Furuichi, P. Furuichi M Fau - Xu, T. Xu P Fau - Tsuzuki, M. Tsuzuki T Fau - Sekiguchi, Y. Sekiguchi M Fau - Nakabeppu, Y. Nakabeppu, Ogg1 knockout-associated lung tumorigenesis and its suppression by Mth1 gene disruption, Cancer Res. 63 (2003) 902–905.
[48] L. Aguilera-Aguirre, A. Bacsi, Z. Radak, T.K. Hazra, S. Mitra, S. Sur, A.R. Brasier, X. Ba, I. Boldogh, Innate inflammation induced by the 8-oxoguanine DNA glycosylase-1-KRAS-NF-κB pathway, J. Immunol. 193 (9) (2014) 4643–4653.
[49] J.B. Spinelli, H.A.-O. Yoon, A.A.-O. Ringel, S. Jeanfavre, C.A.-O. Clish, M.A.-O. Haigis, Metabolic recycling of ammonia via glutamate dehydrogenase supports breast cancer biomass, Science 358 (2017) 941–946.
[50] M.A.-O. Sullivan, L.V. Danai, C.A.-O. Lewis, S.H. Chan, D.Y. Gui, T. Kunchok, E. A. Dennstedt, M.A.-O. Vander Heiden, A.A.-O. Muir, Quantification of microenvironmental metabolites in murine cancers reveals determinants of tumor nutrient availability, Elife (8) (2019), e44235.
[51] R.P. Soultanakis, R.J. Melamede, I.A. Bespalov, S.S. Wallace, K.B. Beckman, B. N. Ames, D.J. Taatjes, Y.M.W. Janssen-Heininger, Fluorescence detection of 8-oxoguanine in nuclear and mitochondrial DNA of cultured cells using a recombinant Fab and confocal scanning laser microscopy, Free Radic. Biol. Med. 28 (6) (2000) 987–998.
[52] X. Yu, Y. Zhang, T. Li, Z. Ma, H. Jia, Q. Chen, Y. Zhao, L. Zhai, R. Zhong, C. Li, X. Zou, J. Meng, A.K. Chen, P.L. Puri, M. Chen, D. Zhu, Long non-coding RNA Linc-RAM enhances myogenic differentiation by interacting with MyoD, Nat. Commun. 8 (2017) 14016, 14016.
[53] X. Ba, A. Bacsi, J. Luo, L. Aguilera-Aguirre, X. Zeng, Z. Radak, A.R. Brasier, I. Boldogh, 8-Oxoguanine DNA glycosylase-1 augments proinflammatory gene expression by facilitating the recruitment of site-specific transcription factors, J. Immunol. 192 (5) (2014) 2384–2394.
[54] L. Huang, C. Zhang, Microscale thermophoresis (MST) to detect the interaction between purified ProteinPurified proteins and small MoleculeSmall molecules, in: G.R. Hicks, C. Zhang (Eds.), Plant Chemical Genomics: Methods and Protocols, Springer US, New York, NY, 2021, pp. 187–193.
[55] M.-C. Sincennes, C.E. Brun, A.Y.T. Lin, T. Rosembert, D. Datzkiw, J. Saber, H. Ming, Y.-i. Kawabe, M.A. Rudnicki, Acetylation of PAX7 controls muscle stem cell self-renewal and differentiation potential in mice, Nat. Commun. 12 (1) (2021) 3253.
[56] C.A. Schneider, W.S. Rasband, K.W. Eliceiri, NIH Image to ImageJ: 25 years of image analysis, Nat. Methods 9 (7) (2012) 671–675.